Tiago Pinheiro Infante

Licenciado em Ciências da Engenharia de Materiais

Optimizing the osteogenic potential of electrospun PVDF matrixes

Dissertação para obtenção do Grau de Mestre em Engenharia de Materiais

Orientador: Prof Dra. Maria do Carmo Henriques Lança, Professora Auxiliar, Universidade Nova de Lisboa

Coorientador: Prof. Dr. João Paulo Miranda Ribeiro Borges, Professor Auxiliar, Universidade Nova de Lisboa

Júri

Presidente:	Prof. Dr. João Pedro Botelho Veiga
Arguente:	Prof. Dr. Rui Alberto Garção Barreira do Nascimento Igreja
Vogal:	Prof Dra. Maria do Carmo Henriques Lança

FACULDADE DE CIÊNCIAS E TECNOLOGIA
UNIVERSIDADE NOVA DE LISBOA

“*What matters is not what others thing of you but how you think of others*”

-Unknown

Acknowledgments

First I would like to thank my coordinator, Prof. Carmo Lança, for her support and guidance during this period of time. Even though there were some complications and obstacles during the development of this work, I was always able to count on her from debating ideas to a simple conversation.

A thanks to Prof. João Paulo Borges for always being a an awesome teacher and helping all the students in his course, I was very fortunate to have him as a co-coordinator during the development of this thesis and even fortunate still to have as a course coordinator and as a teacher.

….To Prof. Jorge Carvalho Silva for the mentoring during the cellular culture procedures, I was definitely lacking knowledge in this area and definitely learned and benefited a lot from being able to work with you. I really enjoyed the though process during our meetings as well as the music running in the background.

I would also like to thank all other members of the faculty with whom I was able to talk to, debate ideas and that helped me with the necessary tests for the characterization of the fibers, a solution may have not always presented itself but the new perspectives helped me to see things differently and though me a lot.

To my friends, you have always been there since day one, thank you for your advice, unyielding support and for all the laughs and good times we had together, form barbecues to nights spent around a table playing games. I love you for everything big and small and wish you the best in your journeys. And to Teresa, a special thanks for one of the best puns about this thesis "*os polimeros não são de fiar*".

To my family, thank for everything, really, you did so much for me I don't even know, were to start, I hope I didn't let you down and that I may one day repay all the kindness you have showed me.

Finally to Carolina, in the short time we have known each other you have been a huge support and a wonderful company, the day I asked you out to see a movie was the best decision I made. I hope we can see many movies together. Thanks for all the support, fun times and great smiles.

Abstract

With an ageing population, the ability to easily regenerate bone defects in a manner that lessens patient site morbidity takes an even more important toll. As such the development of a biomaterial that is capable of successfully mimicking the native environment encountered in the human body is necessary in order to facilitate the regenerative process.

Since traditional orthopedic materials lack some of the necessary ability to mimic the native environment, new approaches must be taken, in this regard polyvinylidene difluoride (PVDF) presents a novel alternative. Since it can be produced via electrospinning in the form of a non-woven fiber matrix that mimics the morphology of the native extracellular matrix (EMC) as well as being able to simulate electrical signals, due to the appearance of a piezoelectric phase due to the electrospinning process, that act as cues for several cellular and molecular processes, including tissue regeneration. The work developed in this thesis aims to optimize the piezoelectric response under electrical stimulation of the electrospun matrixes by adjusting the spinning parameters in order to device an optimal scaffold for bone tissue growth and regeneration.

Structural analysis of the material, shows that the electrospinning process give origin to a new structural organization. When compared to the original PVDF powder, after processing the polymer presents higher crystallinity and also higher content of the β piezoelectric phase. However no significant differences were found in crystalline phases, porosity and overall crystallinity for samples spun under different conditions.

Cytotoxicity tests shown that PVDF mats present a non-cytotoxic behavior. Cellular tests under electric stimulus showed no statistical difference between samples with higher and lower piezoelectric response. However regardless of the sample type, the cells demonstrate a much higher metabolic activity when had received an external stimulus.

Keywords: PVDF, electrospinning, piezoelectric response, bone tissue, regeneration

Resumo

Com o envelhecimento da população, a habilidade de regenerar defeitos ósseos de forma simples e que evite a morbidade de pacientes toma um papel ainda mais importante. Como tal o desenvolvimento de um biomaterial capaz de imitar com sucesso o ambiente nativo do corpo humano é necessário para facilitar este processo de regeneração.

Uma vez que materiais ortopédicos clássicos não conseguem, de forma eficaz, replicar este tipo de ambiente são necessárias novas soluções, neste âmbito o fluoreto de polivinilideno (PVDF) apresenta uma nova e desejada alternativa. Isto graças à sua capacidade de ser produzido através do processo de electrospinning, o que lhe confere não só uma morfologia semelhante à da matriz extracelular (ECM) mas também a capacidade de simular sinais eléctricos que desencadeiam e participam em vários processos de regeneração celulares, inclusive processos de regeneração de tecido, isto graças ao aparecimento de fases piezoeléctricas criadas no processo de electrospinning.

Uma análise estrutural dos materiais demostrou que o processo de electrospinning dá origem a novas organizações estruturais dentro do material, que após o processo de fiação apresenta novas fases cristalinas e uma maior cristalinidade, quando comparado com o pó de PVDF utilizado para fazer as soluções. No entanto não foram encontradas diferenças significativas para a fases cristalinas, cristalinidade e porosidade apresentadas por membranas produzidas através de processos de fiação diferentes.

Após testes de citotoxicidade, foi visto que o PVDF não era citotóxico e foram iniciados ensaios de cultura celular, mais uma vez não foram encontradas diferenças significativas entre os diferentes grupos quando submetidos a um mesmo estímulo. No entanto as células demonstraram uma actividade metabólica muito superior quando submetidas a um estímulo externo.

Palavras-chave: PVDF, electrospinning, resposta piezoeléctrica, tecido ósseo, regeneração

Contents

List of Tables

List of Figures

Glossary:

Electrospinning – a fiber production method that is able to produce fibers with diameters in the manometer to micrometer scale by means of an electric field application;

Piezoelectricity - a linear electromechanical interaction between the mechanical and electrical states in a material;

Osteoblasts – single nucleus cells that plays a primary role in the synthetization of bone tissue;**Extracellular matrix** – a collection of extracellular molecules secreted by support cells that provides structural and biochemical support to the surrounding cells;

Vero cells – kidney epithelial cells extracted from a *Cercopithecus aethiops;*

P-Value – is the probability for a given statistic model that, when the null hypothesis is true, the statistical summary would be the same or of grater magnitude than the observed results;

F-Value – is the value of the Fisher statistic for the parameters;

Acronyms:

ANOVA – Analysis of Variance;

ABCE – PVDF matrixes spun undre the following conditions : distance to target 10 cm, applied voltage 12 kV, needle gauge 25 G, feeding flux 1 ml/h and a collector rotation of 2500 rpm;

CE - PVDF matrixes spun undre the following conditions : distance to target 15 cm, applied voltage 15 kV, needle gauge 25 G, feeding flux 1 ml/h and a collector rotation of 2500 rpm;

DMF – Dimethylformamide;

DMSO - Dimethyl sulfoxide;

DSC – Differential scanning calorimetry;

ECM - Extracellular Matrix;

FA's – Focal Adhesions;

FBS – Fetal Bovine Serum;

FIB-SEM – Focus Ion Beam Scanning Electron Microscope;

FTIR – Fourier Transformed Infrared Spectroscopy;

MS – Mean Square;

MSC's - Mesenchymal stem cells;

PVDF - Polyvinyldene fluoride;

SS – Sum of Squares;

XRD – X-Ray Diffraction;

List of Symbols

A_j – baseline-corrected absorbance at j cm^{-1} (a.u)

K_i^j – absorbance coefficient at j cm^{-1} for the i phase (μm^{-1})

X_i – mole fraction of the I phase

t – sample thickness (μm)

X_c(%) – percentage of sample crystalinity

H_{fs} – the fusion enthalpy of sample (J/g)

H_{ft} – fusion enthalpy for a 100% crystalline sample (J/g)

$\rho_{fiber\ mat}$, $\rho_{thin\ film}$ – Density of the fiber mat and thin film respectively (g/cm^3)

1. Introduction

1.1. A general view

Tissue engineering is a multidisciplinary branch that combines a variety of different approaches but typically it involves the use of a biomaterial as a scaffold, this biomaterial can then be combined with the use of staminal cells or other types of stimuli to promote its integration and the regeneration of certain biological tissues. [1, 2]

Materials used as scaffolds as for tissue engineering applications are designed to match structural morphological, mechanical and chemical properties of the native tissue. [3]. In this particular case we will study the use of piezoelectric PVDF fiber matrixes and see how electrical signals affects the mineralization process of bone tissue. To this end, the fibers will be produced changing several parameters in the electrospinning process to verify which one yields the best electrical response, the chosen fiber mats will then be characterized through SEM, DSC, FTIR, XRD and biocompatibility and bioactivity will be done with recourse to two bioreactors that allow for electrical stimulation of the membranes and see which ones maximize the biological response of the osteoblasts in *in vitro* conditions.

1.2. Bone, a biological tissue

Bone is described as an interconnected, highly organized, specialized and dynamic tissue made up of metabolically active cells and a vast intracellular matrix made up of collagen fibers and inorganic hardening substances forming a rigid matrix. [4 - 7] Like many of the other tissues present in the human organism, bone as the ability to self-regenerate [8] However in order for this to occur it is necessary to recruit specific mesenchymal cells, with the ability to later differentiate themselves into cells capable of initiating the osteogenic process. This cells *e.g* MSC's, exist in the surrounding tissues as well as in the marrow and play a vital role in the regeneration of bone tissue due to their ability to differentiate into different types of biological tissues. [9, 6]

1.3. Fracture healing an overview

It is safe to assume that the regenerative potential of bone is strongly dependent on a series of biochemical, biomechanical, cellular, hormonal and pathological factors. [4, 8]

After a lesion, tissue regeneration occurs in three distinct but overlapping steps this being, inflammation, repair and remodeling [7] represented in figure 1.

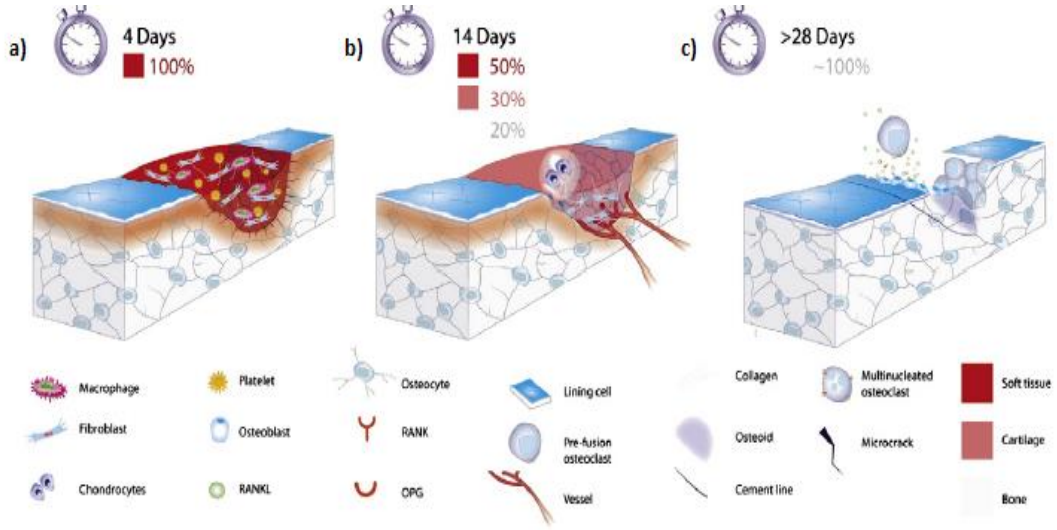

Fig. 1 – Temporal progression of fracture healing, illustrating the, inflammatory, repair and remodeling steps as well as the cells and biological mechanisms participating in the healing process. (taken from [7])

- In the first stage, figure 1-a there is an acute inflammatory reaction and creation of a hematoma around area that suffered trauma. In an early stage the hematoma constricts the blood vessels around the injured area cutting the blood flow to the injury, this creates a rise in local pressure that results in a mechanical stimulus that facilitates the production of an ECM rich in fibrin, necessary for tissue repair. At a later time in the inflammatory stage, as the blood clots dissolve, begins the angiogenesis [7, 8];

- During the repair stage of fracture healing, figure 1-b vascular growth continues aided by the fibroblasts. As vascular growth progresses a collagen matrix is deposited forming a soft callus around the healing tissue, this callus however does not possess the mechanical properties of the original tissue and calcifies, in a period of 4 to 6 weeks, forming a bridge that connects the non-matured tissue to the fracture fragments [7, 8];

- Total fracture regeneration only occurs during the remodeling stage of the healing process, figure 1-c the callus fully calcifies and suffers and osteoclastic remodeling, leading to a fully matured tissue that can now assume his former functions [7, 8].

1.4. The use of biomaterials

As it was seen fracture healing is not only a long and arduous process it is also intrinsically complex as many types of cells and growth factors are involved in the process [8] furthermore, this process can be even more adverse or even be made impossible without external aid if, e.g the patient suffers from bone disease like osteoporosis or in lesions above a critical size [7]. In cases such as this the use of grafts becomes necessary.

Bone grafts can be autologous, when they come from the patient, however this come with several disadvantages due to the fact that additional surgery is required to remove the graft from the patient, which in itself incurs several risks and extends the recovery time for the patient also the quantity of bone that can be extracted to make a

graft is limited. As an alternative to autologous bone grafts there are also homologous bone grafts, this ones come from third parties such as cadavers, removing the risks of an additional surgery but bring different set of problems to consider, such as the possibility of infection and patient rejection. Taking these facts into account, synthetic bone grafts present a viable and appealing alternative. [10 - 13]

1.5. Piezoelectricity in bone tissue

Bone is a dynamic tissue in constant adaptation and remodeling through complex feedback mechanisms, involving electro-mechanical processes, due to its piezoelectric characteristics. The mechanical stress produces electrical signals and these signals represent a stimulus that promotes bone growth and remodeling according to Wolff's law. [14]

In 1892, Julius Wolff postulated that the remodeling of bone tissue architecture occurred as a response to mechanical stimuli, Wolff's Law. [15] The piezoelectric effect plays an important physiological role when it comes to bone tissue growth. In the 60's it was observed that bone tissue presented a low piezoelectric coefficient (≈ 0.7 pC/N) and that it derived from small mechanical stimuli, manly from the collagen fibers sliding against one another.[16] After this discovery piezoelectricity was the phenomenon used to describe bone growth and reabsorption in response to a mechanical stimulus.

Basset and Becker latter described Wolff's Law as a loop of negative feedbacks, where an applied physical load causes tension along the bone, this tension is felt in the less dense and therefore softer areas of the bone in a greater extent than it is felt in the harder and denser areas. The strain is then transformed into an electric field that gadders and aligns ions and macromolecules, e.g Ca^{2+} and PO_4^{3-} existing in the ECM attracting them to the pole with the opposite charge, stimulating bone tissue growth and regeneration and promoting favorable graft/patient interactions. [17]

It is the safe to say that changes in the surrounding environment act as stimuli that are first translated as an electric response that triggers certain cellular events that are key to the regeneration process. [18] [14]

1.6. Piezoelectric scaffolds

Piezoelectric scaffolds present a novel and exciting prospect in the field of tissue engineering thanks to their intrinsic properties. Piezoelectric materials are capable of producing an electric charge when receiving a small mechanical stimulus similar to the ones found in a dynamic *in vivo* environment. [1] This allows piezoelectric materials to simulate biological cues hence promoting greater cellular growth and differentiation when compared to non-piezoelectric materials. [19] However there are still other parameters to take into account in regards of patient-graft interaction, for the graft to be accepted by the host, favorable biomaterial/cell interactions must occur. [8]

Ideally the biomaterial is not just accepted and tolerated by the surrounding environment, it much more desirable that the material plays an active role in the biological events providing an appropriate environment that allows for proper cellular adhesion and signaling. [20, 21]

As such, electrospun polymeric membranes present a very attractive option for tissue engineering applications. Polymers present very attractive properties when compared to inorganic materials. They are light, inexpensive, mechanically and electrically tough, they show excellent compatibility with other organic and inorganic materials. [14]

By utilizing the electrospinning technique we are able to obtain non-woven fiber mats, with fibers as small as a few dozen nanometers in diameter. These fiber mats mimic the ECM exceptionally well as they are highly porous, said porosity is interconnected and present a very large surface area to volume ratio, making them ideal for cell adhesion, differentiation and proliferation. [20, 6, 22] Further more altering the production parameters such as applied voltage, distance to the collector, polymer concentration, polymer flow rate and ambient humidity change the mats morphology, topography and porosity. [23]

In particular altering the applied voltage and polymer concentration have a strong effect in fiber size and morphology [20, 24, 25] making them parameters of vital importance seeing how membrane topography and fiber morphology have a direct impact on cells cytoskeleton being capable of altering the cells own deformability. [5] Further adding to these parameters importance is the fact that osteoblasts are cells that are anchorage dependent, meaning that they can only proliferate when attached to the substrate. [20, 6, 26, 3] Adding to its processing advantages, the electrospinning technique allows for further post-processing refining of the obtained mats allowing them to be customized with the desired cues for triggering and guiding cellular events. [21, 27, 3]

1.7. Polyvinyldene fluoride

Polyvinyldene fluoride, PVDF, $(-CH_2-CF_2-)_n$ is a semi-crystalline biopolymer with excellent mechanical properties, an high chemical resistance, good thermal stability and excellent electroactivity. [26, 28] PVDF can be processed in order to present four crystalline phases α, β, δ and ϒ depending on the processing conditions.

Since the hydrogen atoms are positively charged and de fluoride atoms are negatively charged, PVDF is inherently polar. However, the net polar moment of the material in its original state is zero due to the random orientation of the individual crystallites, however permanent dipole polarization of PVDF is obtained through mechanical stretching of the polymer. Stretching provides a preferential alignment of the molecular chains, [29] in this particular case stretching is obtained by the electric field generated during the electrospinning process.

The β-phase has an all-trans (TTT), planar conformation, figure 2-b giving a higher permanent dipole and as a result better electroactive properties when compared to the other phases and therefore is the most desirable phase for this types of applications [28, 30], this change in conformation can be brought about by mechanical stretching inherent to electrospinning process, in this case mechanical stretching was obtained using an electrospinning process coupled with a rotating collector drum [27]. This type of behavior can also be found in the δ and ϒ phases but to a lesser extent were as the α phase presents a trans-gauche (TG+TG-) conformation, figure 2-a making the dipoles in the monomers to face in opposite directions and thus resulting in a non-polar crystal.

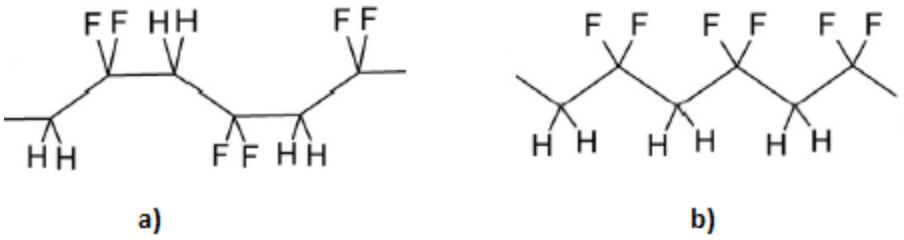

Fig. 2 – Different phases of Polyvinyldene fluoride a) α-phase conformation were the dipoles face in opposite directions, b) β-phase conformation showing a permanent dipole (adapted from [17])

Cellular adhesion is considered one of the most important factors when it comes to cell/biomaterial interactions. [27] Focal adhesions (FA's) are predominant mechanism by which the cells physically connect and interact with the ECM, comprised of extracellular molecules that act as structural and biochemical support for the surrounding cells and contains cues that act as stimuli that trigger biological events. [2, 21, 31] As such the development of a biomaterial that can successfully mimic the native ECM and direct cellular events is a fundamental component in tissue engineering.

In the direct piezoelectric effect an electric potential is generated in response to a mechanical solicitation. In the inverse piezoelectric effect an electrical charge produces a mechanical response in the material. Studies have showed that the surface charge present in these types of substrates coupled with their ability to mimic the mechanical and electrical stimuli present in the human body, has a great influence in certain cellular behaviors such as cell adsorption, proliferation, differentiation and growth. [20, 7, 17, 24]

As such PVDF's intrinsic properties and adding the fact that it can be produced by means of electrospinning, make this material a prime candidate for applications in tissue engineering.

From what could be found in the literature many studies regarding the use of stimulus as a method do enhance cellular activity have already been done [1] [7], however the study, shown in this paper, of how the electrospinning parameters can be used to maximize the piezoelectric response of a fiber matrix and how in turn this translates to cellular behavior was not found in the literature and seems to be a pertinent approach to this types of studies.

2. Materials and methods

2.1. Summary

During the course of this thesis the production method of electrospun PVDF fiber mats was optimized in an attempt to create a fiber mat that could maximize the osteogenic response of osteoblastic cells. To this end several parameters such as polymer concentration, applied voltage, needle gauge, distance to the target and target rpm's were tested. The chosen fiber mat was then characterized and underwent a series of tests to evaluate its viability in tissue engineering applications.

2.2. Scaffold fabrication

Polyvinyldene fluoride (Mw = 534 000 g/mol; #MKBY6618V Sigma-Aldrich) was mixed with acetone (#S7BED73SV Sigma-Aldrich) and Dimethylformamide (1719239 Fisher Chemical) in order to produce an array of solutions with concentrations spanning form 17 to 21 % (wt/v) at two different solvent ratios, these being 6:4 and 1:1 of DMF to acetone respectively [1] [24].

The polymer solutions, were left mixing on a heating plate at a temperature of approximately 75°C over a period of 48 h in order to obtain a homogenous solution and were then spun using the experimental set-up illustrated in figure A1.1 and the experimental conditions described in table 1.

Table 1 - Experimental setup used in preliminary electrospinng experiments

Applied voltage (kV)	Distance to target (cm)	Flow rate (ml/h)	Deposition time (min)	Needle Gauge	Air humidity (%)	Temperature (°C)
15	15	1	30	23	45 – 50	21 ± 3

This preliminary spinning process with a static collector, covered in aluminum foil was used to determine which solvent ratio was most suited for the desired application, this evaluation was made using SEM analysis.

After determining the most suited solvent ratio the solutions were then spun using the experimental set-up illustrated in figure A1.2, this time to evaluate which polymer concentration was best suited for the desired applications.

The polymer solutions were then spun in the same conditions as those shown in table 1 except this time a rotating collector drum, spinning at 2000 rpm was used. It is important to note that this time an accurate measurement of air humidity and room temperature was not possible since the system is not in an isolated chamber as the previous one.

Once again an evaluation of the fibers morphology and topography was made using SEM analysis.

2.2.1. Spinning parameters

The choice of the spinning parameters was made by choosing five different parameters at two different levels each, following a classical experimental design, DOE, with the

intent of maximizing the mats piezoelectric response. The chosen parameters and their respective high and low levels are shown in table 2

Table 2 - Chosen parameters and respective level values for the electrosping parameters

Levels	A – Distance to target (cm)	B – Applied voltage (kV)	C – Needle gauge	D – Flow rate (ml/h)	E – Targets rotation (rpm)
High (+)	10	12	25	0.5	2500
Low (-)	15	15	23	1.0	2000

2.2.2. Scaffold characterization

Scanning electron microscopy (FIB-SEM) Zeiss Auriga microscope with an acceleration voltage of 5 kV was used to characterize the fibers in regards to their morphology and topography.

X-ray diffraction (XRD) measurements were made using an X´pert Pro from Panalytical, utilizing $Cu_{K\alpha}$ radiation (λ = 0.154 nm) an electrical current of 40 mA and a voltage of 45 kV, a step of 2Θ = 0.02 and a step time of 1.0 s was used to characterize the fibers on their crystalline organization.

Fourier-transform infrared spectroscopy (FTIR) was used to characterize the chemical bonding structures. Measurements were made using an Attenuated Total Reflectance (ATR) sampling accessory (Smart iTR) equipped with a single bounce diamond crystal on a Thermo Nicolet 6700 Spectrometer. The spectra were acquired with a 45° incident angle in the range of 4500–525 cm^{-1} and with a 4 cm^{-1}resolution In addition tapping tests were also used to characterize the fiber mats as to their piezoelectric response, this test were first made using single impact with a free falling object dropped from a fixed high and at a later date using a tapping machine to generate impacts at a fixed frequency of 1 Hz, the machine used was developed by Nuno Pinela [32].

2.4. Cytotoxicity tests

To ensure that the material was fit to support cellular growth and differentiation cytotoxicity tests were conducted using Vero cells in accordance with the ISO 10993-5 standard using the extract method. To this end 70 mg of spun material were sterilized using a 70% ethanol solution which was left to evaporate over a period of 48 h.

The material was then submerged in 2ml of culture medium consisting of , DMEM (Dulbecco′s Modified Eagle′s Medium, Sigma-Aldrich #D5030) supplemented with 1.0 g/L D-glucose (Gibco, #15023-021), 3.7 g/L sodium bicarbonate (Sigma-Aldrich, #S5761), 1% GlutaMAX™ (L-alanyl-L-glutamine dipeptide, Life Technologies, #35050-038), 1% sodium pyruvate (Gibco, #11360039), penicillin (100U/ml) and streptomycin (100 µg/mL) (Invitrogen, #15140122), 10% FBS (Fetal Bovine Serum, Invitrogen, #10270106).

The extracts were prepared by placing the material in contact with medium without FBS under orbital shaking in an oven at a temperature of 37°C. After 48h, 910µL

of extract was supplemented with 90 µL of FBS. The cell cultures were prepared in a 96 multiwell plate, 6000 cells per well, 24h before receiving the extracts, five rows of five wells were prepared. The first row received extract corresponding to a concentration of 35 mg/mL. Then, the extract was diluted by a factor of 2 for the second row of wells and this process was repeated until a dilution factor of 16 was reached for the wells in the fifth row.

In addition, two columns made up the positive control, were cells were killed using a 10% DMSO solution, and a negative (non-cytotoxic environment) control. Material cytotoxicity was evaluated using a medium solution prepared with 50% of a 0.04 mg/ml resazurin solution in PBS and 50% of complete culture medium. After an incubation period of 2h, the absorbance was read at 570 nm and at 600 nm to calculate the amount of resazurin metabolized in to resorufin and from these values calculate relative (to the negative control) cell viability in each experimental condition. All measurements were obtained using an ELx800 from BioTek.

2.5. Cellular response tests

One of the primary difficulties in evaluating the premise that a higher piezoelectric response is translated in higher cell activity, is that since osteoblasts are anchorage dependent, altering the morphology and topography of the substrate, as well as the crystalline phases present in the sample will influence molecular response. Many approaches were attempted, such as thermal ageing of the samples, in order to achieve an identical subtract in terms of morphology and topography but with no piezoelectric response. However since the Curie temperature of PVDF is far above its melting temperature any attempt to depolarize the samples, by disorganizing the preferential dipole orientation in the sample, resulted in a great deformation and alteration of the substrate. As such the chosen solution was to use samples that underwent different spinning conditions, and as such have different piezoelectric responses.

To evaluate the manner in which cells interacted with the electrospun matrixes and to see if the premise that a higher piezoelectric response did in fact yield better results in terms of cell adhesion, proliferation and ultimately osteogenic growth was valid, three sets of six samples were taken from two fiber matrixes spun in different conditions, and that exhibited very different electrical responses when submitted to a mechanical stimulus, the samples produced under the conditions ABCE ($A^+B^+C^+E^+$) presented a much higher electrical response when compared to samples spun under the CE (C^+E^+) conditions, table 3. These samples were also submitted to an alkaline phosphatase test to evaluate their metabolic response [6]. The test are made by introducing p-nitrophenylphosphate (pNPP) to the culture medium that has alkaline phosphatase, an enzyme produced by the cells that will degrade the pNPP yielding p-nitrophenol, a chromogenic product that has a yellow color. The absorbance at 405 nm is then measured and compared between samples and a control group

In addition in order to see the effect of a dynamic stimulus environment two samples one spun in ABCE conditions, which showed a maximized response, and a sample spin under conditions CE, randomly chosen, were taken and placed in separate bioreactors and underwent a stimulation of 1.5 V at 1 Hz, in an attempt to characterize the cellular behavior when cells were put under the influence of an external stimulus and in the presence of an electroactive matrix with different piezoelectric responses. The bioreactor was developed by Carlos Marques (MSc thesis in biomedical engineering FCT/UNL, to be submitted). The stimulus was applied for 1 h periods every 12 hours. If

any significant cellular behavior changes were detected this could then in turn be attributed to the difference in piezoelectric response shown by the spun matrixes.

.

3. Results and discussion

3.1. Choosing a solvent ratio

After the preliminary electrospinning process, using the static set-up the samples underwent SEM analysis to verify the fibers morphology, figure 3.

From the SEM images shown in figure 3 it is visible that a solvent ratio of 6:4 creates a more disperse array of fibers rather than an interconnected highly porous matrix when compared with a solvent ratio of 1:1. Despite the presence of beads for lower concentrations for a solvent ration of 6:4, a solvent ratio of 1:1 was chosen in the experimental works.

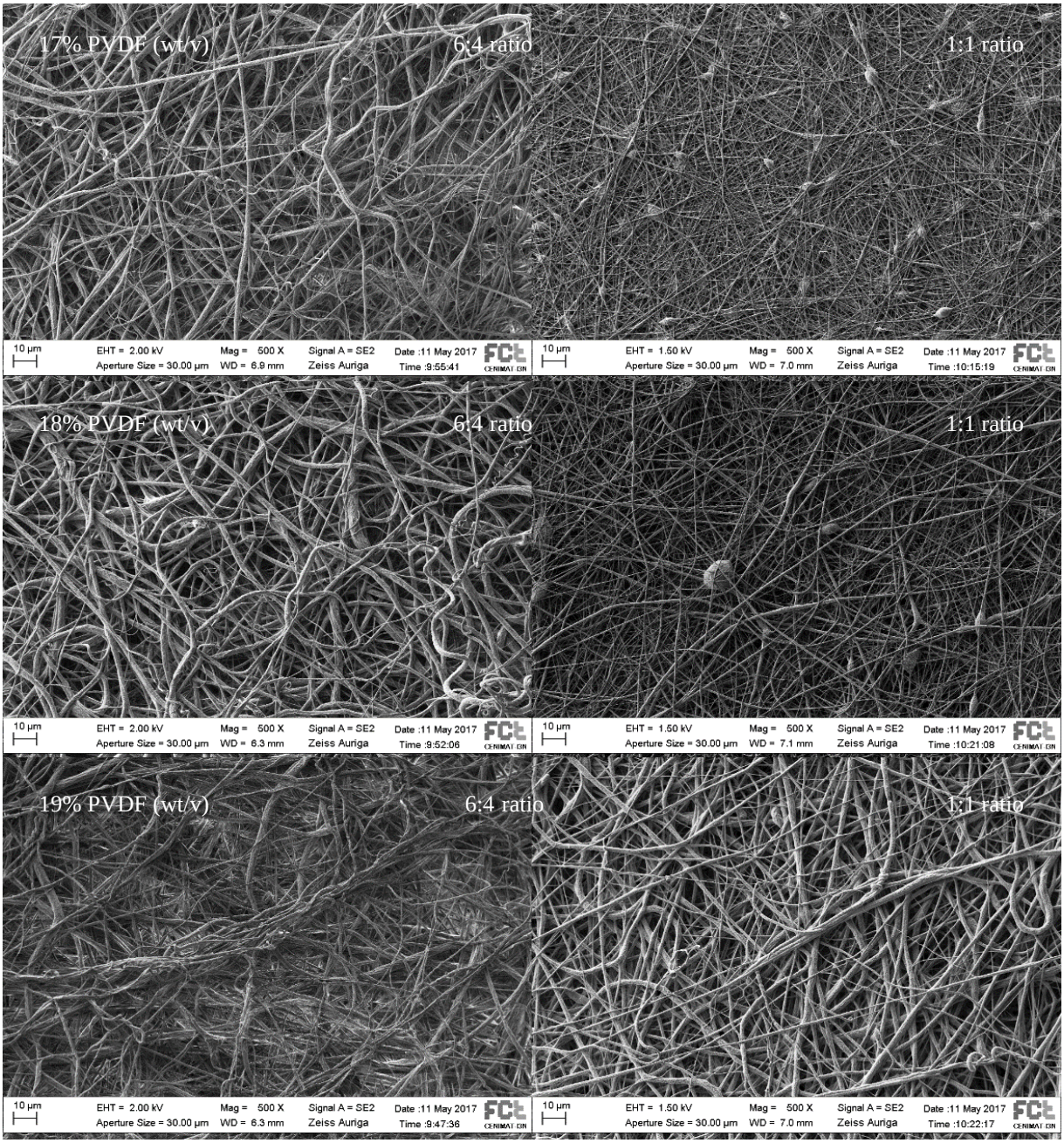

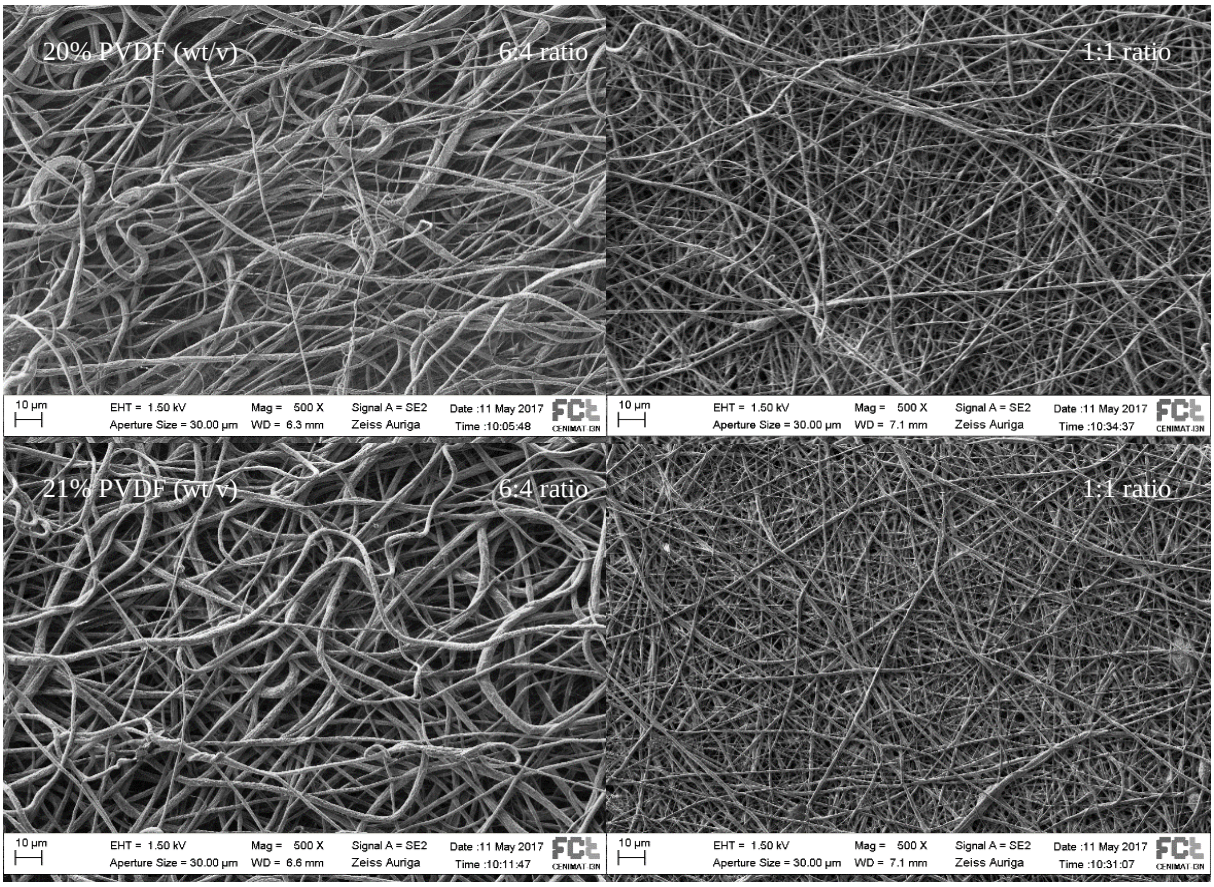

Fig. 3 - SEM images at 500x amplification obtained from the electrospun PVDF fibers for different concentration and solvent ratios. On the left side are the solutions spun with an 6:4 DMF to acetone ratio and on the rigth the solutions spun with and 1:1 DMF to acetone ratio. The polymer concentration grows from top to bottom from 17 to 21%

3.2. Choosing a polymer concentration

After the spinning processes illustrated in figure A1.2 the fibers were again analyzed with recourse to SEM imaging, figure 4.The SEM analysis shows that visible structural defects such as beads lessen as polymer concentration increases. As such a polymer concentration of 21% was chosen for the next set of experiments.

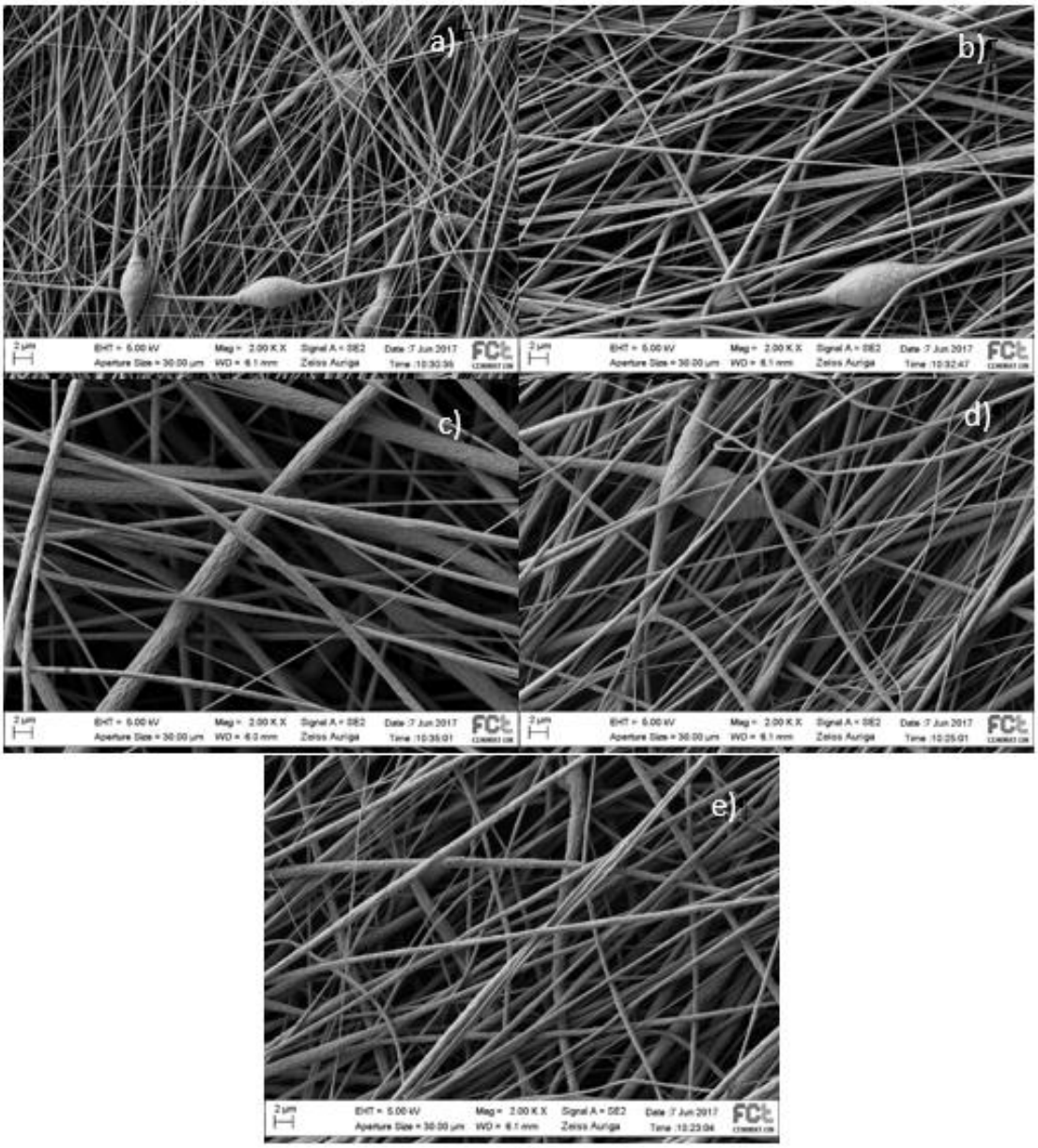

Fig. 4 - SEM images at 2000x amplification of the aligned fiber mats obtained using the experimental set-up illustrated in figure A1.2. a) 17%; b) 18%; c) 19%; d) 20% and e) 21% polymer solution with a solvent ratio of 1:1

3.3. Piezoelectric tests

All the 32 samples produced, with approximately 300 μm thickness, were submitted to single impact test in order to evaluate if a piezoelectric response existed, the test was performed by dropping a 15.17 g object from a 20 cm height on to a sample connected to a Hantek6022BE PC-Oscilloscope and measuring the electrical response given, data not shown. All samples produced an electrical response, and as such were submitted to tapping tests under dynamic mechanical stimulation.

All of the 32 samples were submitted to a dynamic mechanical stimulation test, using a Tektronix TDS 2001C oscilloscope; at a frequency of 1Hz to evaluate which yielded the best electrical response. A complete factorial design was implemented, resulting in a total of 2^5 experiments presented in the planning matrix shown in table 3.

The experiments were done, three times, in a random order to assure that all observed results are independent events. [32]

For the following calculations only the highest voltages measured in a peak was accounted for and not the voltage peak to peak, figure 7 , this is because most of the waves were asymmetric and the smallest peaks were often not measurable due to background noise, with some exceptions.

The results of the experiments as well run order in which the experiments were conducted are shown in the following table, where + represents the high level of given factor and - represents the low level of a given factor. According to table 2.

Table 3 – Table showing the run order of the experiments consisting in a dynamic stimulation of the membranes at 1 Hz

RUN ORDER	A	B	C	D	E	PEAK VALUE AT 1,0 HZ (V)	JOHNSONS TRANSFORMATION
1	+	-	+	+	+	0,8	-0,287
2	-	+	+	-	+	1	0,097
3	-	-	+	-	+	0,29	-2,557
4	+	-	-	+	+	0,56	-0,920
5	+	+	+	+	-	0,6	-0,793
6	-	+	-	+	+	0,72	-0,470
7	-	-	-	+	+	2,1	1,648
8	+	+	+	+	+	0,72	-0,470
9	-	-	+	+	+	0,56	-0,920
10	-	-	+	-	-	0,76	-0,376
11	+	+	-	+	-	1,3	0,570
12	-	+	+	+	-	0,8	-0,287
13	-	-	+	+	-	2	1,512
14	+	-	+	+	-	1,9	1,379
15	-	+	+	-	-	0,7	-0,519
16	-	+	+	+	+	0,52	-1,060
17	+	-	-	-	-	6,4	-
18	-	-	-	-	+	2	1,512
19	+	+	+	-	-	1,3	0,570
20	+	+	-	+	+	1,4	0,712
21	+	-	-	-	+	0,68	-0,570
22	-	+	-	-	-	1,4	0,712
23	+	-	-	+	-	1,3	0,57
24	-	+	-	-	+	1,1	0,265

25	+	+	-	-	+	0,68	-0,570
26	-	-	-	-	-	1,4	2,085
27	-	-	-	+	-	0,8	-0,287
28	+	-	+	-	+	0,4	-1,611
29	+	+	+	-	+	1,5	0,849
30	+	+	-	-	-	0,6	-0,793
31	+	-	+	-	-	0,4	-1,611
32	-	+	-	+	-	1,1	0,265

The data was then analyzed using the software Minitab®, a preliminary look at the data, utilizing an Anderson-Darling test for a significance level of 0.05 revealed that the residuals did not follow a normal distribution as shown in figure A2.1, in annex 2.

With a p-value < 0.005 we reject the null hypothesis that the data is normally distributed, and as such an analysis of variance, ANOVA, is not possible. However it is also shown in figure.5 that only one result greatly escapes normality. That value corresponds to the residual of the experiment 17 in the run order, highlighted in red, table.3. To see if this result could be excluded from further calculations an outlier test, Grubb's test, with a significance level of 0.05 was used, figure.A2.2 in annex 2.

It is evident using this test that the value obtained in experiment 17, table 3, is an outlier and as such it will not come into consideration in any further calculations nor experiments. An additional Anderson-Darling test, with a significance level of 0.05 was performed in the data residuals after removing the outlier, figure.A2.3 in annex 2.

The Anderson-Darling test presented in figure A2.3, in annex 2, shows a p-value > 0.005 and as such we do not reject the null hypothesis and can assume that the residual data follows a normal distribution however the p-value for the Anderson-Darling test just barely meets the requirements for normality and further analysis shows that the residues may actually have a non-homogeneous variance as shown in figure A2.4, in annex 2, when plotted against the fitted values they seem to form a cluster around 0.9 to 1.35.

As such a Johnson's transformation was performed on the data, table 3 a new analysis was performed on the residuals of the transformed data figure 5 and figure 6.

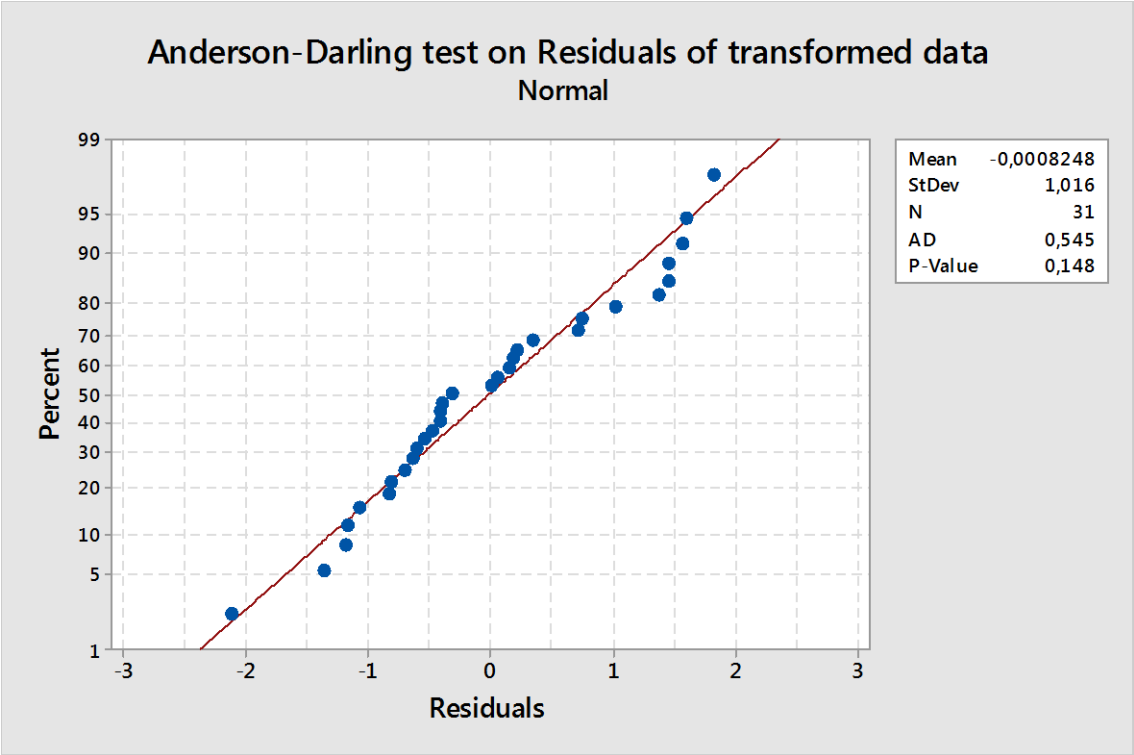

Fig. 5 - Graphic representation of an Anderson-Darling test with a significance value of 0.05 on the data residuals after a Johnsons tranformation

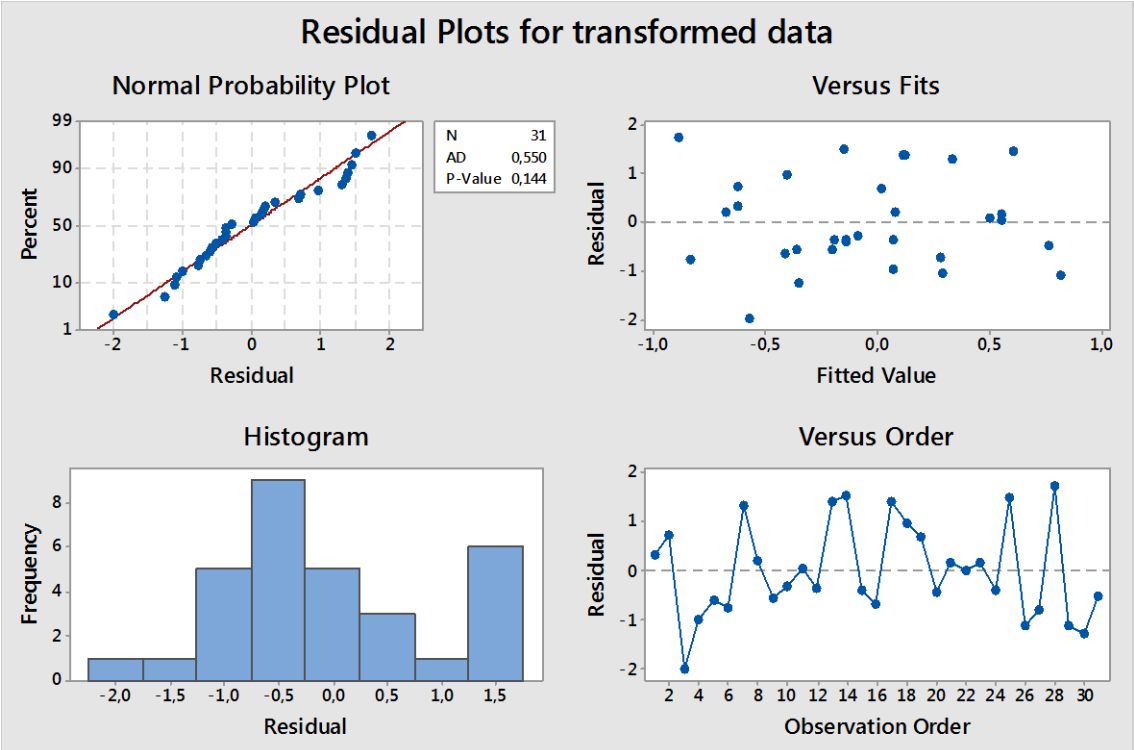

Fig. 6 - Residual plots for transformed data showing how well they fit a normal distribution, their order versus the run order and their variance when compared with the fitted values as well as an histogram of their distribuition

The residuals for the transformed data now show much higher p-value in the Anderson-Darling test meaning that they better fit a normal distribution, figure 5 when compared with the non-transformed ones shown in figure A2.1, in annex 2, in addition it is now safe to say that none of the principles of normality are being broken, the residuals are now normally distributed, they are independent form each other and they seem to present a homogenous variance, figure 6, and as such an analysis of variance ANOVA using the transformed data, table 4, to determine the combination of levels that maximizes the fiber mats piezoelectric response is now possible.

Table 4 – ANOVA with a significance level of 0.05 utilizing the transformed data

Source	Degrees of freedom	SS	MS	F-Value	P-Value
A	1	0.5435	0.54353	**0.50**	0.488
B	1	0.0211	0.02114	0.02	0.891
C	1	3.7502	3.75020	**3.42**	0.076
D	1	0.3337	0.33372	0.30	0.586
E	1	1.7819	1.78193	**1.63**	0.214
Error	25	27.3838	1.09535		
Total	30	33.9136			

After the ANOVA analysis it is visible that for a significance value of 0.05 factors A, C and E have a significant impact in the piezoelectric response of the fiber mats.

The best combination of levels is then determined by adding the contributions of the significant effects, highlighted in green in table 4, at both high and low levels, this being represented by ∑ (+) and ∑(-) respectively and choosing the ones with the highest value since the goal is to maximize the piezoelectric response.

Table 5 - Table showing the added contributions of the significant effects at both levels.

	∑(+)	**∑(-)**
A	-2.975	1.620
C	-6.084	4.729
E	-4.352	2.997

According to results shown in table 5 the best levels for the effects that have a significant effect in the response are A^+, C^+ and E^+ for all other effects that do not have a significant influence in the response their levels can be chosen in a way that they are more convenient for the research, usually they are chosen based on how affordable they are but since that parameter holds no weight in this particular case the final combination of levels was chosen based on the registered responses shown in table 3.

As such the combination of levels chosen in the experiments moving forward was $A^{+}B^{+}C^{+}D^{-}E^{+}$ with a registered response of 1.5 V for a stimulation of 1 Hz, figure 7 c). The sample $C^{+}E^{+}$ was used as comparison and its results are shown in figure 7 b) and 7 d).

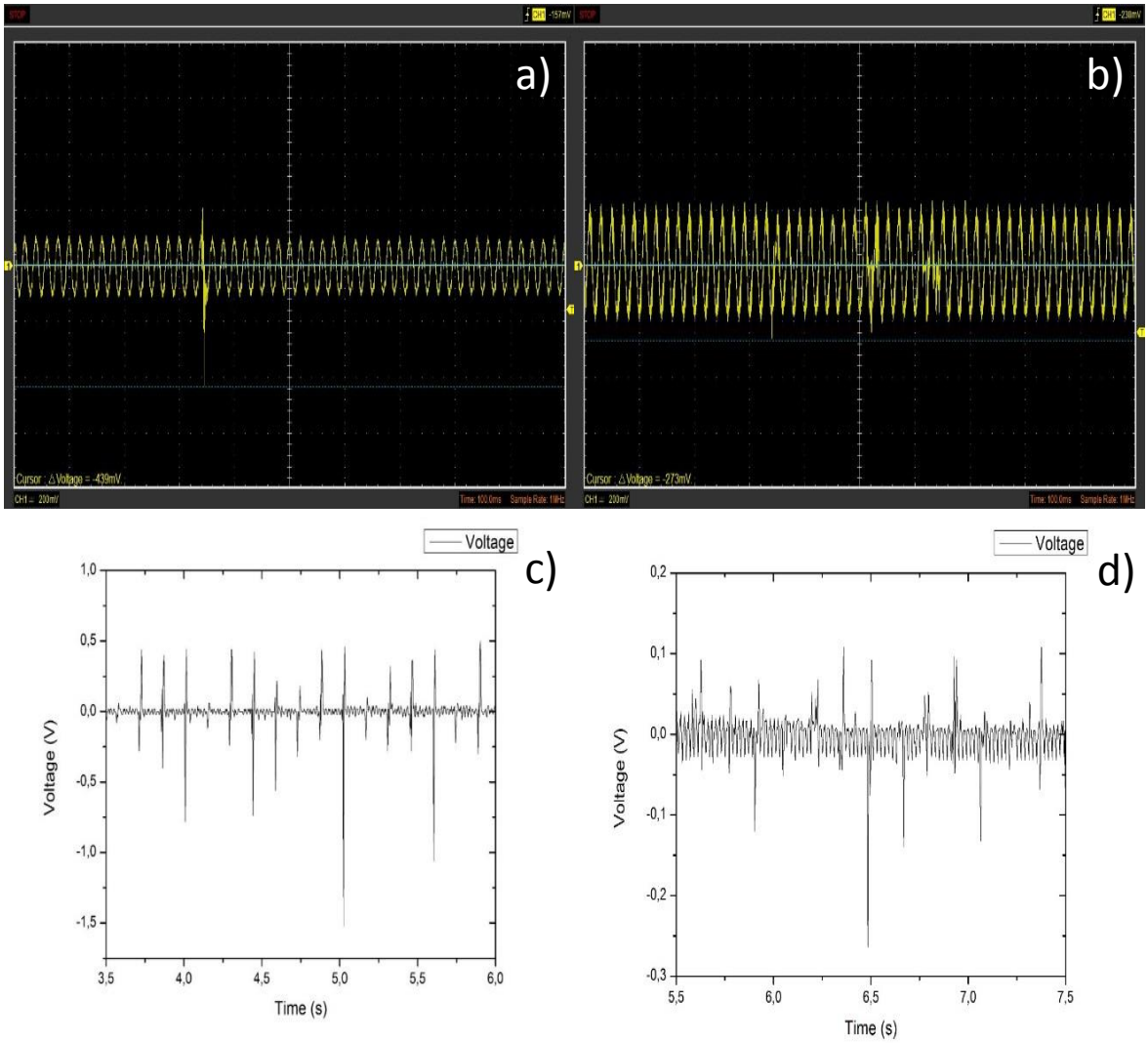

Fig. 7 – a) piezoelectric response for single impact test in a fiber matrix spun in ABCE conditions, with a response of -0.439 V, b) piezoelectric response for single impact test in a fiber matrix spun in CE conditions, with a response of -0.273 V, c) piezoelectric response for dynamic impact test, at 1Hz in a fiber matrix spun in ABCE conditions, d) piezoelectric response for dynamic impact test, at 1Hz in a fiber matrix spun in ABCE conditions

The measurements were first made using a piece of paper and no response was obtained, this served to prove that the fibers do indeed possess a piezoelectric response, however this does not guaranty an accurate reading since the measurements are made by taking the fibers deposited in an aluminum foil electrode placing an additional electrode on top of the fibers and applying a mechanical solicitation. This in turn can result in a capacitance change due to varying distance of the electrodes can generate artifacts that add to the true output signal. [34] In addition peaks should only show when a mechanical stimulus was applied to the sample, one each second, since the stimulus was done at one Hz, the presence of other peaks can be attributed to the triboelectric

effect, especially when taking into account that the PVDF is negatively charged (due to the fluoride atoms in its composition) when compared whit the aluminum used to make the electrical contacts.

3.4. Scaffold Characterization

3.4.1. XRD characterization

The fiber mat spun under the chosen conditions was analyzed using an X-ray diffraction technique and the data was treated using the OriginPro 8.5 software in order to characterize it taking into account the crystallographic phases present and compare it to the unprocessed PVDF powder used to make the polymeric solutions, figure 8.

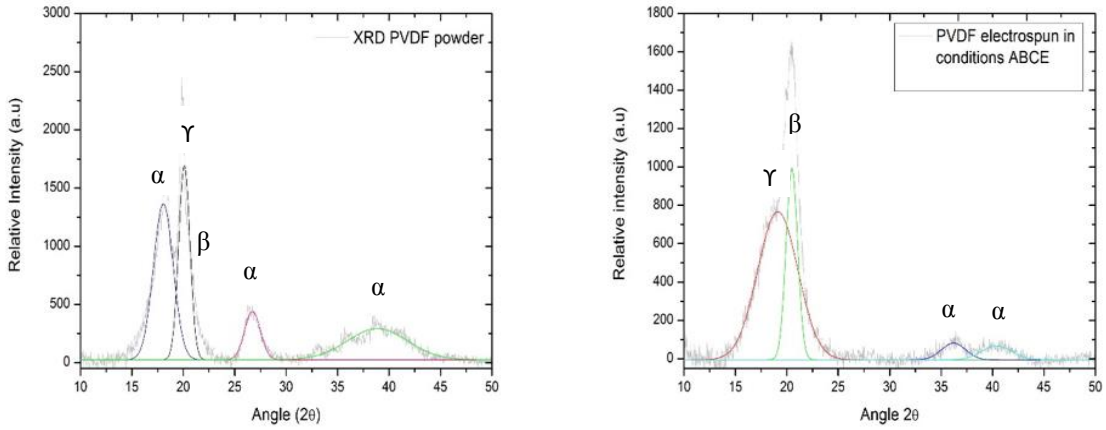

Fig. 8 - XRD difractograms for PVDF samples, on the left the XRD specter for unprocessed PVDF powder and on the right the XRD specter for PVDF spun under the chosen conditions.

Through observation of figure 8 it is visible that the unprocessed PVDF powder shows diffraction peaks at 2Θ = 18.09°, 20.01°, 20.70°, 26.70° and 38.90° corresponding to α-phase (1 0 0)/ (0 2 0), to the ϒ-phase (1 1 0), to the β-phase (2 0 0) to the ϒ-phase (0 2 2) and to the α-phase (0 0 2) reflection planes respectively. [35]

In comparison the electrospun PVDF presents a diffraction pattern with peaks at 2Θ = 19.20°, 20.70° and 36.20° corresponding to the ϒ-phase (0 0 2), the β-phase (2 0 0) and to the ϒ-phase (2 0 0) reflection planes respectively. There is also a diffraction peak at around 2Θ = 40° corresponding to the α-phase (0 0 2) reflection plane. [35]. Showing a much higher content of β piezoelectric phase and a small amount of the non-piezoelectric α phase.

3.4.2. FTIR characterization

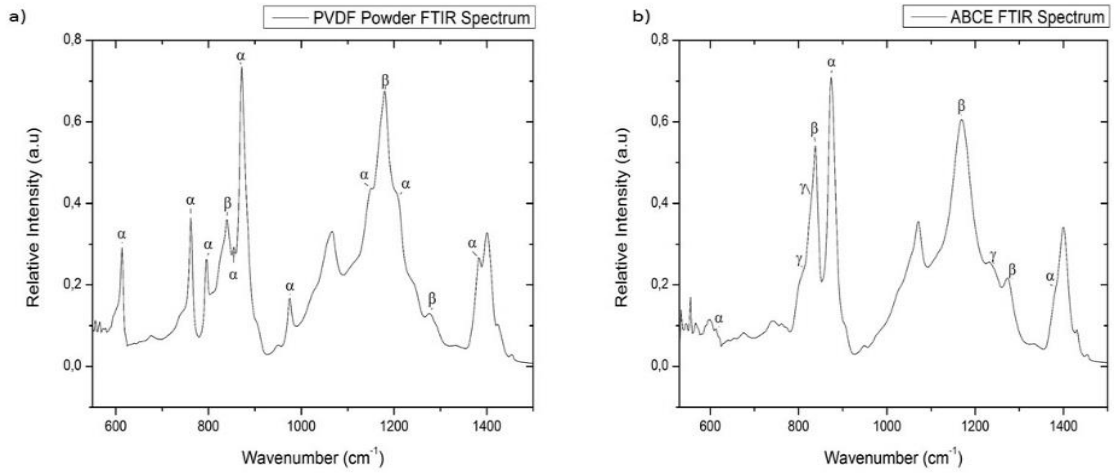

Fig. 9 – FTIR spectra of the unprocessed PVDF powder and the PVDF solution electrospun under the ABCE experimental conditions

It is visible in figures 8 and 9 that the electrospinning process coupled with the mechanical strain from the rotating collector drum creates a crystalline structure much richer in electroactive crystalline phases when compared with the unprocessed PVDF powder. [29, 35] When compared with the electrospun samples unprocessed powder shows peaks of much lower intensity in the β-phase peaks at 838 and 1280 cm^{-1} and a much higher intensity in the α-phase peaks at 612, 761, 795, 1147 and 1211 cm^{-1}. [24] [25] [30] [36]

3.4.3. FIB-SEM characterization

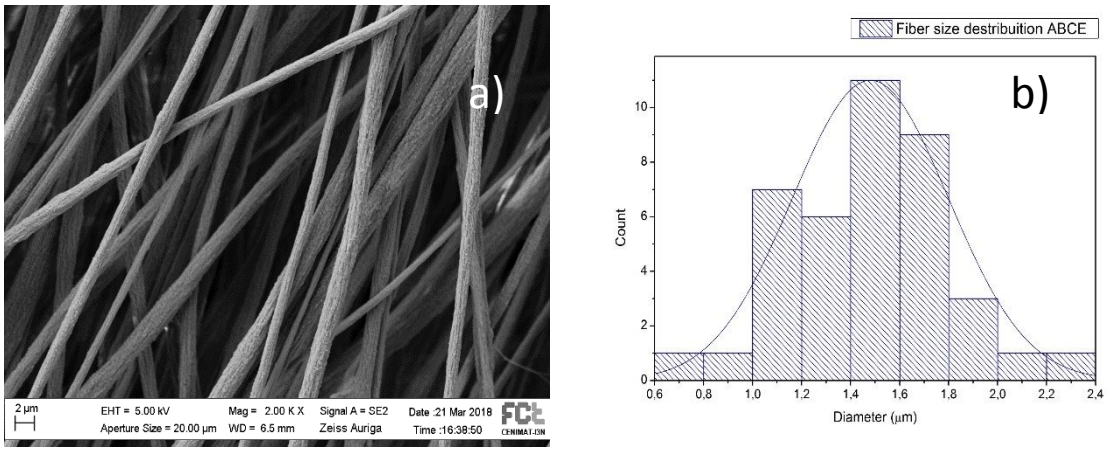

Fig. 10 – a) SEM imaging at 2000x amplification of a fiber matrix electrospun under the conditions ABCE showing a preferential alignment of the fibers; b) Fiber size distribution of 40 counts total and a comparison to a normal distribution fitting

The electrospinning process under the chosen conditions leads to a semi aligned quasi-normal, distribution of the fibers with the bulk of the fibers having between 1.4 and 1.6 µm of diameter, figure 10. Fiber sizes were obtained using the software ImageJ®.

3.5. Cytotoxicity tests

The cytotoxicity tests were performed using the Biotool Vita-blue Cell Viability reagent, this reagent is a redox indicator which utilizes the blue and weakly fluorescent Resazurin reagent to reduce to pink and highly fluorescent Resofurin by dehydrogenase enzymes in metabolically active cells, being that the amount of Resofurin produced is directly proportional to the number of living cells. [37]

It was found that for all concentrations, the concentration to negative control ratio was superior to a 0.9 value meaning that the material was not cytotoxic and as such the material is fit for biological applications. The test sensitivity was also tested using the positive (C+) to negative (C-) control medium ratio and it showed a value 0.023 meaning that the test is indeed sensitive to the Resazurin to Resofurin reduction and not any external factors, both results are shown in figure 11 a) and b) respectively.

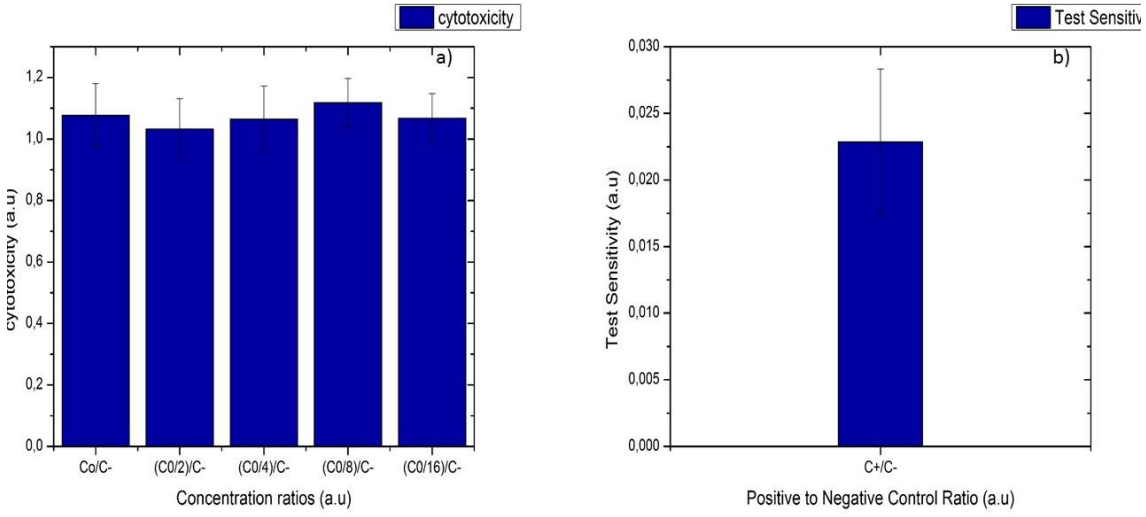

Fig. 11 - a) figure showing the results of the several concentrations to negative control medium ratios, the values over 0.9 show the PVDF scaffolds as a non-cytotoxic medium; b) figure showing the positive (C+) to negative (C-) control ratio, the low value indicates that the test is indeed sensitive to the reduction of Resazuirn and not to external factors.

3.6. Structural characterization

It is important to state that due to the first batches of membranes being too thin thicker membranes with an exposure time of 2 h had to be produce, this in turn makes it so that the response of each of the membranes is not the one viewed in table 3 [38], new testing to assure the membranes response was not possible since there was a malfunction in the necessary equipment.

3.6.1. Comparing sample groups

Using equations 1 through 3 the molar fraction of α and β-phases in each sample can be calculated. [39]

$$A_{762} = k_{\alpha}^{762} * X_{\alpha} * t \ (eq.1)$$

$$A_{1275} = k_{\beta}^{1275} * X_{\beta} * t \ (eq.2)$$

$$A_{1070} = 0.095t + 0.07 \ (eq.3)$$

Where A_j is the baseline-corrected absorbance at j cm^{-1}, k^j_i is the absorbance coefficient at j cm^{-1} for the i phase, X_i is the mole fraction of the i phase and t is the thickness of the sample in μm and it is obtained using the samples absorbance of infra-red radiation at 1070 cm^{-1}seeing as this peak is relatively independent from the samples crystallinity, the values for K_{α}^{762} and K_{β}^{1275} are 0.365 and 0.140 μm^{-1} respectively [39] [40] Results for the mole fractions of each phase are shown in table 6 and the values used for the calculations are presented in annex 3.

Table 6 – Mole fractions of both α and β phases present in the fiber mat samples

	ABCE	CE	PVDF Powder
X_{α}	0.06	0.04	0.34
X_{β}	0.63	0.61	0.21

Through analysis of the FTIR spectra shown in figure 12 it is clear that both samples present a similar spectra meaning that the electrospinning process did not lead to a significant difference in molecular organization when comparing the two samples. The relative fraction of β-phase can be obtained using equation 2, for samples ABCE and CE, at 1275 cm^{-1}, is 63% and 61% respectively. Meaning that modifying the spinning parameters does not have a great impact in the crystalline composition of both samples. However when comparing the spun samples to the original PVDF powder there is a noticeable increase in the amount of β phase and a decrease in the amount of α phase in the samples, verifying that the spinning process leads to a transformation of the non-piezoelectric α phase into other piezoelectric phases more desirable for this kind of applications. Additional information on the vibrational modes of each of them can be found in annex 3.

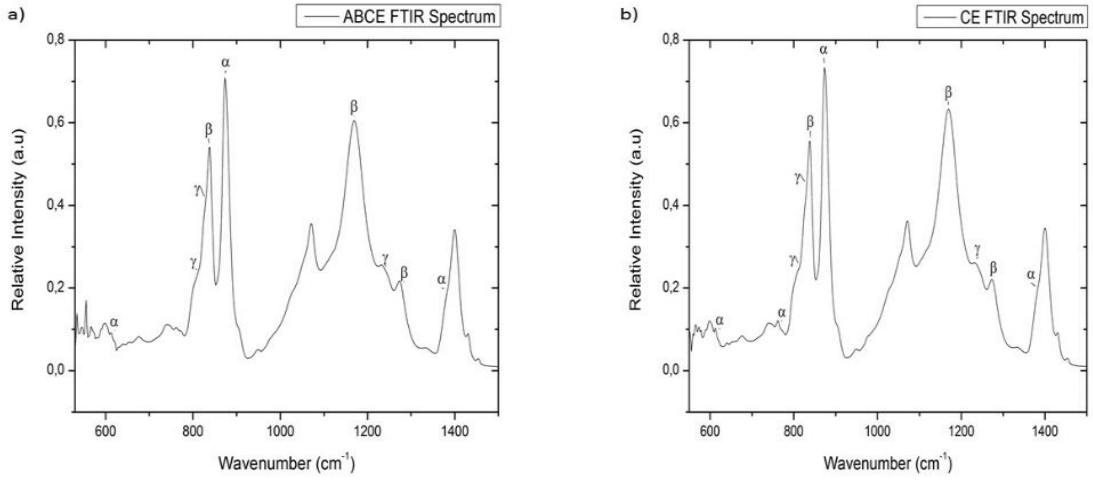

Fig. 12 - FTIR spectra comparing both samples, electrospun under different conditions used in static environment cellular culture test,

From what can be seen in figure 13, both samples present a very similar composition when it comes to the crystalline phases present in them although slight differences can be found. The sample electrospun under the conditions ABCE presents a slightly more intensive and broader peak at 2Θ = 19.20° corresponding to the ϒ-phase (0 0 2) reflection, in addition the peaks at 2Θ = 36.20 and 40°corresponding to the ϒ-phase (2 0 0) and the α-phase (0 0 2) reflection planes respectively, are slightly more prominent in this sample when compared with sample CE. In addition the peak at 2Θ = 20.06° corresponding to β-phase (2 0 0) reflection plane show a much higher intensity in sample ABCE when compared with sample CE. Meaning that the ABCE processing conditions favor the formation of β-phase (2 0 0) reflection plane when compared with the CE processing conditions.

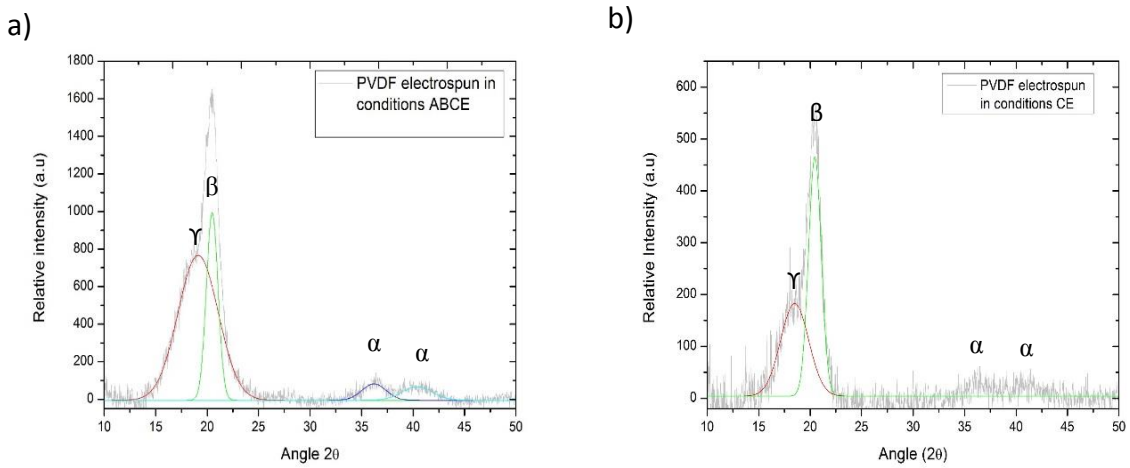

Fig. 13 - XRD difractograms comparing both samples, electrospun under different conditions used in static environment cellular culture tests, a) XRD spectrum of fiber mat spun under the conditions ABCE, b) XRD spectrum of fiber mat spun under the conditions CE

In figure 14 it is presented SEM imaging of both samples ABCE and CE at 2000x amplification, their respective tread count distribution and how well that distribution fits a normal distribution. As it can be seen in figure 14 a), the sample processed under ABCE conditions presents a much more aligned fiber matrix when compared with the sample produced under CE conditions as well as a much more evenly distributed fiber diameter this is of extreme importance since an evenly distributed fiber diameter translates to an evenly distributed fiber mass which in turn translates to a similar resonance frequency throughout the entire device and as such an even response to the electrical stimulus, since the resonance of a piezoelectric material depends on several other factors such as elasticity and dampening effects. As described in Van Dyke's model. [38]

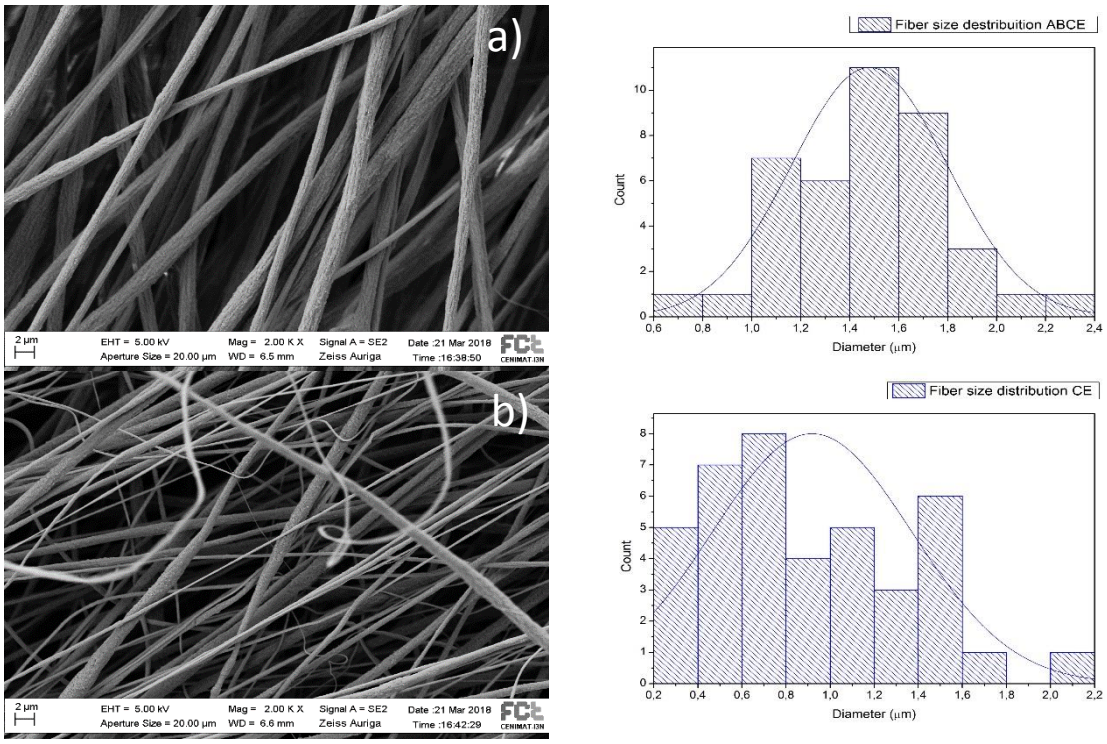

Fig. 14 - – SEM imaging 2000x amplification and tread count distribution, 40 counts per sample, of the fiber diameters in both samples. a) sample electrospun under conditions ABCE, b) sample electrospun under conditions CE

Additionally a DSC scan of the samples was made in order to quantify the samples overall crystallinity using equation 4.[30]

$$X_C(\%) = \frac{H_{fs}}{H_{ft}} * 100 \ (eq. 4)$$

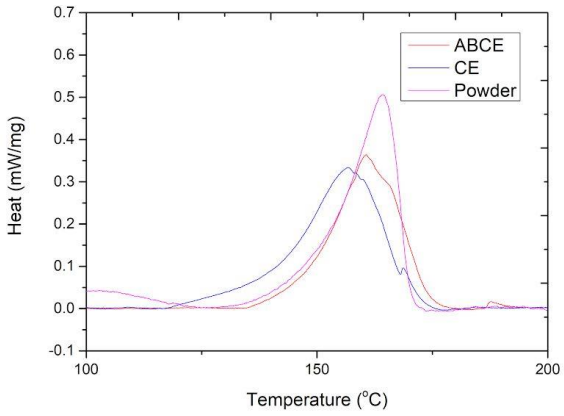

Fig. 15 - DSC scan of all samples showing their primary melting peaks (endothermic peaks) at around 160 °C

Where H_{fs} the area beneath the primary melting peak for each sample, when plotting the heat flux data vs time , (in s), figure not shown, and corresponds to the fusion enthalpy of sample in J/g, H_{ft} is the fusion enthalpy for a 100% crystalline sample, in case of β-

PVDF this value is 104.6 J/g, the value for both α and ϒ-PVDF samples is unknown and is assumed as being the same as β-PVDF, following the work of Prest and Luca. [30][39][40] Results for sample crystallinity can be seen in table 7.

Table 7 – Degree of crystalinity of each sample using the primary melting peak of each sample

	Powder	ABCE	CE
X_c(%)	38.2	44.6	44.9

Finally, using equation 5 both of the fiber mats porosities were calculated and compared. To evaluate the scaffolds as to their porosity, thin films of PVDF with the same concentration were produced. The solution was poured on to glass plaques and left to dry at a temperature of approximately 90°C to ensure the formation of a dense film. [40]

$$Fiber\ mat\ porosity\ (\%) = \left(1 - \frac{\rho_{fiber\ mat}}{\rho_{thin\ film}}\right) * 100\ (eq. 5)$$

Both samples presented very similar degree of porosity being that the ABCE samples and the CE samples presented (98.1 ± 0.2) % and a (98.0 ± 0.2) % respectively. Which means that the change in spinning parameters did not change the overall porosity of the fiber mats. All this factors in conjunction with the preferential alignment of the fibers could explain the superior response from part of the fiber matrixes produced under ABCE conditions.

3.7. Cellular response tests

3.7.1. Static tests

Three sets of twelve membranes each (six of each type ABCE and CE) were seeded with a cell density of 20 000 cells/ cm^2 and the adhesion of the cells was evaluated 24 h hours after the seeding was done and the proliferation of said cells was evaluated every two days for a period of 9 days after culture. It is of note that both experiments one and three had to be terminated due to unforeseen complications, and as such only the result from the second experiment will be presented.

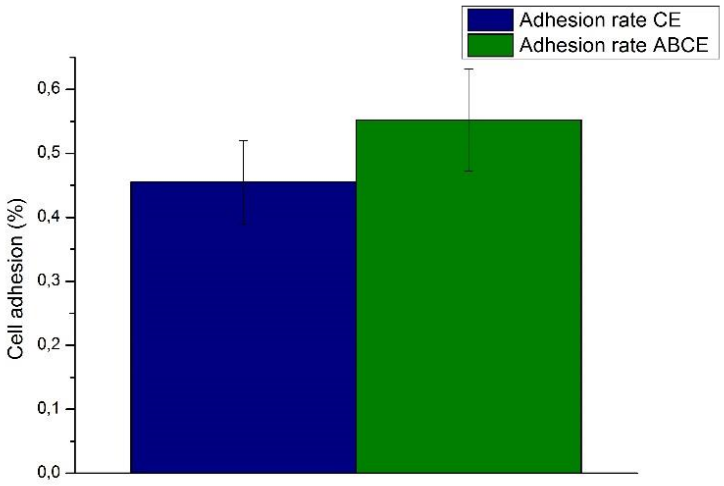

Fig. 16 - Comparison of cellular adhesion betwen fiber matrixes during the second set of experiments

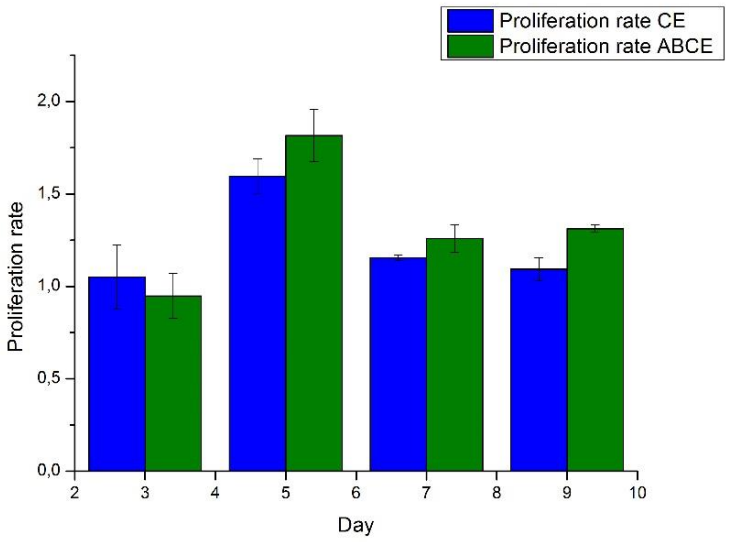

Fig. 17 - Comparison of cellular proliferation rate between fiber matrixes in static regime during the second set of experiments

From the data shown in figures 16 and 17 it is visible that the fiber matrix produced under the ABCE electrospinning conditions presents a higher adhesion and proliferation rate when compared to the ones produced under the CE electrospinning parameters. It is important to note that in experiments 1 and 3, data not shown, the CE group presented a higher adhesion rate than the ABCE sample but still with no significant differences between the two groups.

To verify if the data is statistically significant, a t-student statistic, with, a significance level of 0.05 and equal variance between samples was used from day 1 (adhesion) to day 9 of the experiment. A chi-square statistic can be found in annex 4, showing that the variance is not significantly different for both samples in the same days,

however, one should note that in the last days of the experiment the p-value is close to 0.05 meaning that for a larger population the samples could in fact present different variances at later stages. The t-student statistic, showed no significant differences between the proliferation rates of both sample groups in the 1st and 3rd days (p-value > 0.05) however subsequent measurements show significant differences between both sample groups proliferation rates (p-value < 0.05) with this difference being statistically more significant as time passes. [33]

Cellular metabolic activity was measured at day 7 for both samples via an alkaline phosphatase test [6] these tests showed no statistical differences between the two samples and show little increase in metabolic activity when compared with the control medium, figure 18.

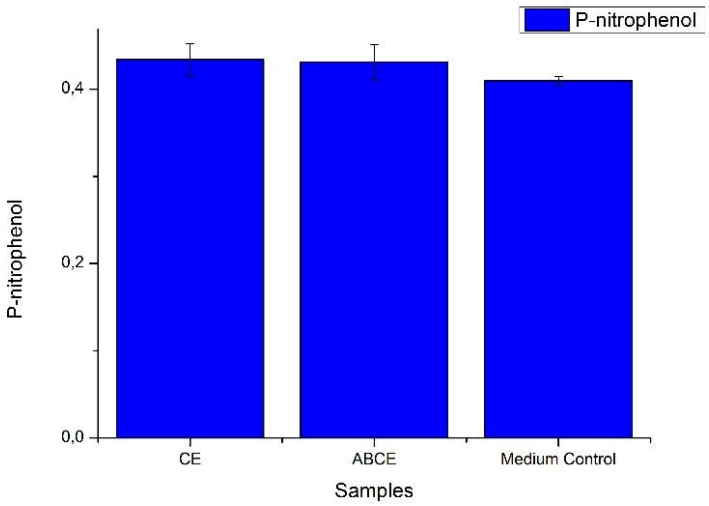

Fig. 18 - *p*-nitrophenol present in both samples and in the control group at day 7 of the experiment

It is visible from figure 18 that for a static regime there are no significant differences between the two groups when it comes to cell metabolic activity for a significance level of 0.05. [33] Equal variance was verified between all groups and is presented in annex 5.

3.7.2. Dynamic tests

The evaluation of cellular behavior in a dynamic environment proved to be a challenge, and several adaptations were made to the procedure and to the bioreactor itself, of the later the most important was the creation of a new orifice near the edge of the lead of the bioreactor, this allows for a proper medium change without the need to remove several components of the bio reactor which in turn create less disturbances in the culture environment. The Teflon ring was also changed for one with 17 and 24 cm of internal and external diameter respectively and a thickness of 1.5 mm.

As for the procedure, the one yielding the best results consisted in the seeding of cell using 500 µl of a solution with a cell concentration of 60 000 cells/ml, in an already fully assembled bioreactor. The use of such low volume assured that the cells would deposit themselves fully in the electrospun matrix and not in other areas of the bioreactor, as figure 19 a, shows, only 1% of the deposited cells did not reach the matrix and were instead deposited in the metallic net. After seeding the cells were left to adjust to their

new environment over a 24 hour period in a controlled atmosphere before any further tests were conducted. After the 24 h period and for all subsequent medium changes, the volume of fresh medium used was of 1 ml, to ensure the cells remained metabolically active. It is of note that between medium changes, and after tests, the samples were washed using a DMS solution to ensure no previous residue remained. An image of the used bio reactors is presented in annex 6.

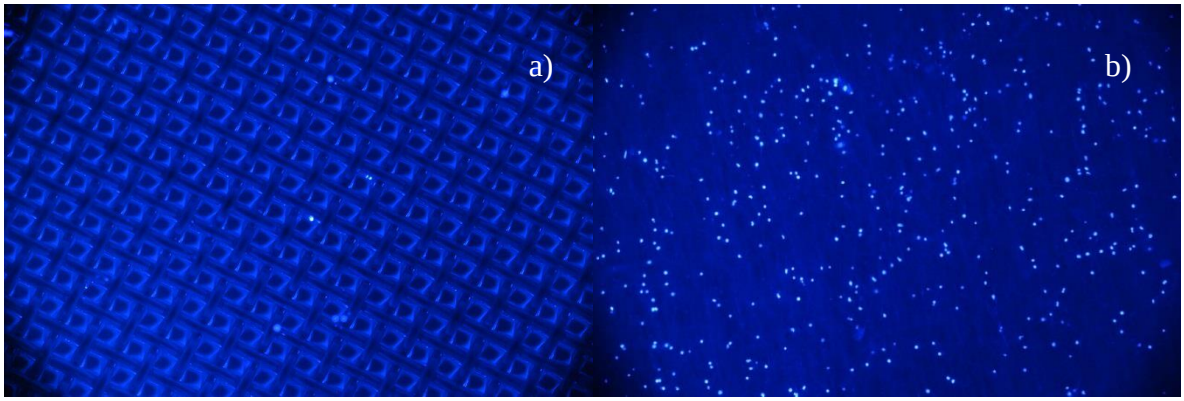

Fig. 19 - Microscopic imaging of the deposited cells, a) view of the metalical net of the bioreactor; b) view of the spin matrix

As was done for the static environment cell proliferation, figure 20 and cellular metabolic activity, figure 21 were evaluated.

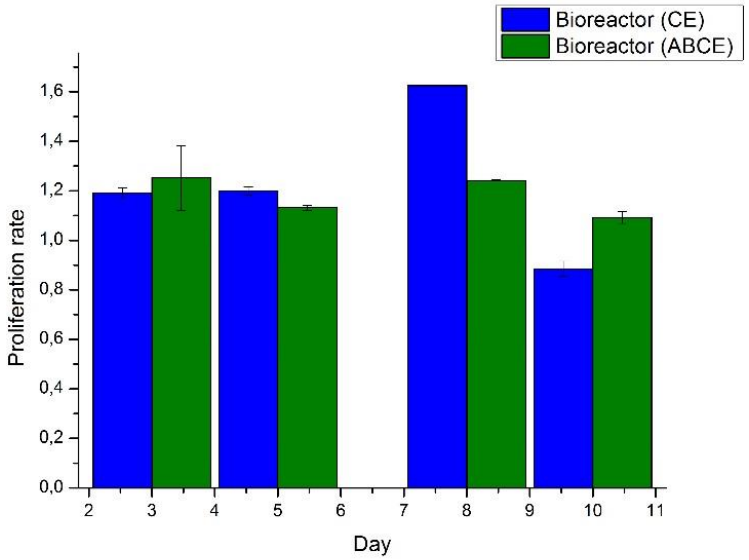

Fig. 20 - Cellular proliferation rate for a five day period without a stimulus application, and for the subsequent days with the application of a 1 Hz, 1.5 V stimulus

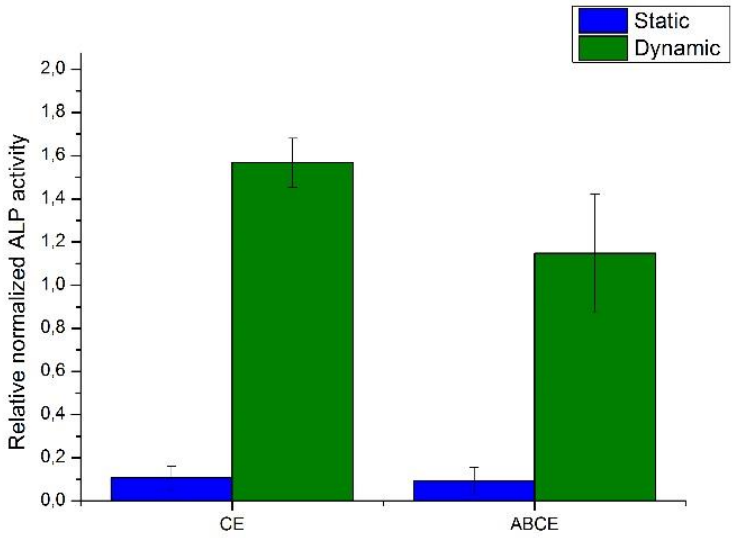

Fig. 21 - Normalized metabolic activity for cells seeded in both ABCE annd CE spun samples and for static and dynamic environments

As seen in figure 20 there is no significant difference, for a significance level of 5%, between the proliferation rate of cells when comparing a static or a dynamic environment, this figure, however, shows an increase in the proliferation rate at day 8, after the cells had undergone 3 days of stimulus, followed by a decrease in the proliferation rate, day 10, to levels more in accordance with the previously seen, this shows that the procedure is still in a very early stage and that are still outside factors interfering with cellular behavior.

When comparing metabolic activity of cells, figure 21, shows the normalized metabolic response of the cells. It is clearly visible that while no significant differences can be found in cellular activity for cells seeded in matrixes either spun in ABCE or CE conditions, there is a clear increase in the metabolic activity of cells when exposed to the stimulus provided in the dynamic environment.

4. Conclusions and future prospects

XRD and FTIR results demonstrated that the electrospinning process coupled with the mechanical strain from the rotating collector drum did alter the structural organization of the samples when compared to the original unprocessed powder sample (higher β and lower α phase contents). In addition the DSC analysis showed an increase in the crystalline fraction of both samples when compared with the unprocessed powder. This findings would suggest that the electrospinning process facilitates the orientation and packaging of the polymer chains by coulombic forces exerted in the process enhancing piezoelectric properties.

Comparing the both spun samples (ABCE spun with a distance between the needle tip and the collector of 10 cm, an applied voltage of 12 kV, a needle gauge of 25G a flow rate of 1 mL/h, a collector drum spinning at 2500 rpm and CE spun with a distance between the needle tip and the collector of 15 cm, an applied voltage of 15 kV, a needle gauge of 25g, a flow rate of 1 mL/h and a rotation of the collector drum of 2500 rpm), the XRD spectra are very similar the difference being that the peaks appearing in at 2Θ = 36.2° and 40° (ϒ-phase (2 0 0) α-phase (0 0 2) reflection planes) present in the ABCE sample seem to be of a more residual nature in the sample spun under the CE conditions. Both samples present almost identical FTIR spectra and the relative fraction of β-phase is, as expected, also very similar. The ABCE sample presenting a mole fraction of β-phase of 63.0% to the 61.0% shown by the CE sample. This fact suggests that, although the electrospinning process does have a great impact in changing the crystallographic phases present in the original PVDF powder, changes in the spinning parameters did not have such a great impact in the crystallographic phases present in the final spun samples. This lead us to infer that the difference between piezoelectric responses in both samples is due to the superior fiber orientation shown by the ABCE samples as well as a more uniform fiber size distribution as shown in figure 14. This allows for a better alignment of the dipoles that translates to a more uniform and greater piezoelectric response.

Ideally the cellular response tests would be performed using matching samples in terms of morphology and topography and the only difference between them would be the piezoelectric response so that any variation in results could be attributed to this factor alone. However it has already been demonstrated that both sample groups present a different topography, and since osteoblasts are anchorage dependent this factor has a great influence in the way they behave. Cellular adhesion tests showed no significant differences between samples, this was also seen in cellular proliferation tests but only during the first days, from days to 5 to 9, after culture, cell proliferation took place at a higher rate in samples from the ABCE processing group, if this in large part because of the difference in piezoelectric coefficients or due to the different fiber sizes distribution still remains unknown. On the seventh day of the experiment an alkaline phosphatase test was done to measure the metabolic activity of the cells in each group, for a static regime there do not appear to be any significant differences between both groups, even between the samples and the control group there is not a significant difference, for a significance value of 0.05, two reasons were considered for this, either there were not enough cells in the groups to make a significant difference when compared with the control group or there could still be residue of previous washing processes done when the medium that feeds the cells is changed. This residue dilutes the total concentration in each well and could in theory influence the readings.

For the future of this project there are a couple of paths to take, the first one is to repeat the spinning and selection processes but this time with deposition times of 2h since it is now known that shorter deposition times produce membranes that are too thin to be handled and tested in the cell culture. Another way to measure the piezoelectric response, preferably through the reverse effect (an electrical stimulus producing a mechanical response) would be a real step forward since this would allow for much accurate readings as it would remove the artifacts created by the impact in the contacts that is present in the measurements here presented and could even allow for a direct measurement of the piezoelectric coefficient d33. Also would allow for a better choice in parameters to use in dynamic tests (voltage and frequency of the signal). Several attempts were made to this end but with no reliable results, several substrates with different conductivities were used to deposit the fibers and this were the taken to undergo AFM analysis but no response was obtained, an impedance measurer was also used but the weight of the contacts was to big when compared to the of the fibers and did not allow them to freely vibrate when stimulated, an attempt to try and measure differences in the optic path of a laser using the department of material science optic bench was also tried but the fibers didn't have a reflective enough surface.

There does not seem to be a significant difference, for a significance level of 0.05, between cellular behavior in both groups, but there is a significant increase in the metabolic activity of cells when comparing static and dynamic tests, the later presenting a much higher metabolic activity. However since the medium is in contact with metallic parts the stimulus will not only be felt by means of a piezoelectric response but also by means of electrical conduction through the medium as well, this presents a novel problem, to be solved since there will always be an electrical stimulus present in the bioreactor environment despite of the sample presenting a piezoelectric response or not. As such any differences in cell behavior cannot be solely attributed to a piezoelectric response, there will be a need to quantify how much of the differences is created by the current in the medium and how much of it is due to the piezoelectric response of the material, for this a bioreactor with a different design may be necessary, in order to try and apply a stimulus only through a piezoelectric response.

5. References

[1] Ribeiro, C., Pärssinen, J., Sencadas, V., Correia, V., Miettinen, S., Hytönen, V. P., & Lanceros-Méndez, S. (2015). Dynamic piezoelectric stimulation enhances osteogenic differentiation of human adipose stem cells. *Journal of Biomedical Materials Research - Part A*, *103*(6), 2172–2175. https://doi.org/10.1002/jbm.a.35368

[2] Obradovic, B. (2012). *Cell and Tissue Engineering*. https://doi.org/10.1007/978-3-642-21913-9

[3] Ribeiro, C., Correia, D. M., & Botelho, G. (2015). Piezoelectric poly (vinylidene fluoride) microstructure and poling state in active tissue engineering.

[4] Kalfas, Iain, H. (2001). Principles of bone healing. *Neurosurgical Focus*, *10*(4), E1. https://doi.org/10.3171/foc.2001.10.4.2

[5] Zhang, Y., Chen, L., Zeng, J., Zhou, K., & Zhang, D. (2014). Aligned porous barium titanate/hydroxyapatite composites with high piezoelectric coefficients for bone tissue engineering. *Materials Science and Engineering C*, *39*(1), 143–149. https://doi.org/10.1016/j.msec.2014.02.022

[6] Yoshimoto, H., Shin, Y. M., Terai, H., & Vacanti, J. P. (2003). A biodegradable nanofiber scaffold by electrospinning and its potential for bone tissue engineering. *Biomaterials*, *24*(12), 2077–2082. https://doi.org/10.1016/S0142-9612(02)00635-X

[7] Fernandez-Yague, M. A., Abbah, S. A., McNamara, L., Zeugolis, D. I., Pandit, A., & Biggs, M. J. (2015). Biomimetic approaches in bone tissue engineering: Integrating biological and physicomechanical strategies. *Advanced Drug Delivery Reviews*, *84*, 1–29. https://doi.org/10.1016/j.addr.2014.09.005

[8] Bab, I. A., & Sela, J. J. (2012). *Principles of Bone Regeneration*. https://doi.org/10.1007/978-1-4614-2059-0

[9] Marsell, R., & Einhorn, T. A. (2011). The biology of fracture healing. *Injury*, *42*(6), 551–555. https://doi.org/10.1016/j.injury.2011.03.031

[10] Ong, J. C. Y., Kennedy, M. T., Mitra, A., & Harty, J. A. (2012). Fixation of tibial plateau fractures with synthetic bone graft versus natural bone graft: A comparison study. *Irish Journal of Medical Science*, *181*(2), 247–252. https://doi.org/10.1007/s11845-011-0797-y

[11] Pilliar, R. M., Kandel, R. A., Grynpas, M. D., & Hu, Y. (2013). Porous calcium polyphosphate as load-bearing bone substitutes: In vivo study. *Journal of Biomedical Materials Research - Part B Applied Biomaterials*, *101 B*(1), 1–8. https://doi.org/10.1002/jbm.b.32832

[12] Heise, U., Osborn, J. F., & Duwe, F. (1990). Hydroxyapatite ceramic as a bone substitute. *International Orthopaedics*, *14*(1990), 329–338. https://doi.org/10.1007/BF00178768

[13] Kotwal, A., & Schmidt, C. E. (2001). Electrical stimulation alters protein adsorption and nerve cell interactions with electrically conducting biomaterials. *Biomaterials*, *22*(10), 1055–1064. https://doi.org/10.1016/S0142-9612(00)00344-6

[14] Ribeiro, C., Sencadas, V., Correia, D. M., & Lanceros-méndez, S. (2015). Colloids and Surfaces B : Biointerfaces Piezoelectric polymers as biomaterials for tissue engineering applications, *136*, 46–55.

[15] Fang, J., Wang, X., & Lin, T. (2011). Functional Applications of Electrospun Nanofibers. *Nanofibers - Production, Properties and Functional Applications*, 287–326. https://doi.org/10.5772/916

[16] Hastings, G. W., & Mahmud, F. A. (1988). Electrical effects in bone. *Journal of Biomedical Engineering*, *10*(6), 515–521. https://doi.org/10.1016/0141-5425(88)90109-4

[17] Rajabi, A. H., Jaffe, M., & Arinzeh, T. L. (2015). Piezoelectric materials for tissue regeneration: A review. *Acta Biomaterialia*, *24*, 12–23. https://doi.org/10.1016/j.actbio.2015.07.010

[18] Clin Orthop Relat Res. 1977 May;(124):5-8. The classic: *Fundamental aspects* of *fracture treatment* by Iwao *Yasuda*, reprinted from J. Kyoto Med. Soc., 4:395-406, 1953.

[19] Chamay, A., & Tschantz, P. (1972). Mechanical influences in bone remodeling. Experimental research on Wolff's law. *Journal of Biomechanics*, *5*(2), 173–180. https://doi.org/10.1016/0021-9290(72)90053-X

[20] Jang, J. H., Castano, O., & Kim, H. W. (2009). Electrospun materials as potential platforms for bone tissue engineering. *Advanced Drug Delivery Reviews*, *61*(12), 1065–1083. https://doi.org/10.1016/j.addr.2009.07.008

[21] Parssinen, J., Hammarén, H., Rahikainen, R., Sencadas, V., Ribeiro, C., Vanhatupa, S., … Hytönen, V. P. (2015). Enhancement of adhesion and promotion of osteogenic differentiation of human adipose stem cells by poled electroactive poly(vinylidene fluoride). *Journal of Biomedical Materials Research - Part A*, *103*(3), 919–928. https://doi.org/10.1002/jbm.a.35234

[22] Shin, Y. M., Hohman, M. M., Brenner, M. P., & Rutledge, G. C. (2001). Experimental characterization of electrospinning: the electrically forced jet and instabilities. *Polymer*, *42*(25), 09955–09967. https://doi.org/10.1016/S0032-3861(01)00540-7

[23] Pham, Q. P., Sharma, U., & Mikos, A. G. (2006). Electrospinning of polymeric nanofibers for tissue engineering applications: a review. *Tissue Engineering*, *12*(5), 1197–211. https://doi.org/10.1089/ten.2006.12.1197

[24] Weber, N., Lee, Y. S., Shanmugasundaram, S., Jaffe, M., & Arinzeh, T. L. (2010). Characterization and in vitro cytocompatibility of piezoelectric electrospun scaffolds. *Acta Biomaterialia*, *6*(9), 3550–3556. https://doi.org/10.1016/j.actbio.2010.03.035

[25] Kumbar, S. G., James, R., Nukavarapu, S. P., & Laurencin, C. T. (2008).

Electrospun nanofiber scaffolds: engineering soft tissues. *Biomed. Mater.*, *3*, 1–15. https://doi.org/10.1088/1748-6041/3/3/03400288/1748-6041/8/4/045007

[26] Ribeiro, C., Moreira, S., Correia, V., Sencadas, V., Rocha, J. G., Gama, F. M., … Lanceros-Méndez, S. (2012). Enhanced proliferation of pre-osteoblastic cells by dynamic piezoelectric stimulation. *RSC Advances*, *2*(October), 11504. https://doi.org/10.1039/c2ra21841k

[27] Stevens, M. M. (2005). Exploring and Engineering the Cell-Surface Interface. *Science*, *310*(2005), 1135–1138. https://doi.org/10.1016/j.bpj.2010.12.1248

[28] Mohammadi, B., Ã, A. A. Y., & Bellah, S. M. (2007). ARTICLE IN PRESS POLYMER Effect of tensile strain rate and elongation on crystalline structure and piezoelectric properties of PVDF thin films, *26*, 42–50. https://doi.org/10.1016/j.polymertesting.2006.08.003

[29] Vinogradov, A., & Holloway, F. (2016). Electro-mechanical properties of the piezoelectric polymer PVDF, *193*(September). Ferroelectrics, Vol. 226, pp. 169-181 https://doi.org/10.1080/00150199908230298

[30] Damaraju, S. M., Wu, S., Jaffe, M., & Arinzeh, T. L. (2013). Structural changes in PVDF fibers due to electrospinning and its effect on biological function, *45007*. https://doi.org/10.1088/1748-6041/8/4/045007

[31] Michel, G., Tonon, T., Scornet, D., Cock, J. M., & Kloareg, B. (2010). The cell wall polysaccharide metabolism of the brown alga Ectocarpus siliculosus . Insights into the evolution of extracellular matrix polysaccharides in Eukaryotes, 82–97.

[32] Miguel, N., & Pinela, G. (n.d.). Piezoresistive pressure sensor for application in e-skin devices. Universidade Nova de Lisboa, FCT/UNL-DCM, 2017. http://hdl.handle.net/10362/26672

[33] Pereira, Z, L. Requeijo, J, G.Qualidade: Planeamento e Controlo Estatístico de Processos. 2ª Edição. FFCT- Fundação da Faculdade de Ciências e Tecnologia da Universidade Nova de Lisboa: (2012); pag: 111-142, 154-186;

[34] Chang, J., Dommer, M., Chang, C., & Lin, L. (2012). Piezoelectric nanofibers for energy scavenging applications. *Nano Energy*, *1*(3), 356–371. https://doi.org/10.1016/j.nanoen.2012.02.003

[35] Taylor, P., Mokhtari, F., Latifi, M., & Shamshirsaz, M. (2015). The Journal of The Textile Institute Electrospinning / electrospray of polyvinylidene fluoride (PVDF): piezoelectric nanofibers, (September). https://doi.org/10.1080/00405000.2015.1083300

[36] Sencadas, V., & Gregorio, R. (2009). α to β Phase Transformation and Microestructural Changes of PVDF Films Induced by Uniaxial Stretch, (November 2008), 514–525. https://doi.org/10.1080/00222340902837527

[37] Blaen, P. J., Brekenfeld, N., Comer-Warner, S., & Krause, S. (2017). Multitracer Field Fluorometry: Accounting for Temperature and Turbidity Variability During

Stream Tracer Tests. *Water Resources Research*, *53*(11), 9118–9126. https://doi.org/10.1002/2017WR02081

[38] Space Administration. Langley Research Center. Hampton, Virginia 23681-2199. *NASA*/*CR-2001-211225*. *ICASE Report No. 2001-28*. *Piezoelectric Ceramics Characterization*. T.L. Jordan. NASA Langley Research Center, Hampton, Virginia. Z. Ounaies. *ICASE*, Hampton, Virginia. *ICASE*. NASA Langley Research Center.

[39] Benz, M., & Euler, W. B. (2003). Determination of the Crystalline Phases of Poly (vinylidene fluoride) Under Different Preparation Conditions Using Differential Scanning Calorimetry and Infrared Spectroscopy. *Journal of Applied Polymer Science*, *89*, 1093–1100.

[40] Prest, W. M., & Luca, D. J. (1978). The formation of the γ phase from the α and β polymorphs of polyvinylidene fluoride. *Journal of Applied Physics*, *49*(10), 5042–5047. https://doi.org/10.1063/1.324439

[41] Taylor, P., Magalhães, R., Durães, N., & Silva, M. (2010). The Role of Solvent Evaporation in the Microstructure of Electroactive β - Poly (Vinylidene Fluoride) Membranes Obtained by Isothermal Crystallization, (September 2013), 37–41. https://doi.org/10.1080/1539445X.2010.525442

[42] Studies, D. S. C., & Mechanically, O. F. (n.d.). Journal of Macromolecular Science , FTIR AND DSC STUDIES OF MECHANICALLY. *Montana The Magazine Of Western History*, (731840606), 37–41. https://doi.org/10.1081/MB-100106174

6. Annexes

1 – Experimental electrospinning step-ups for static and rotating drum collectors

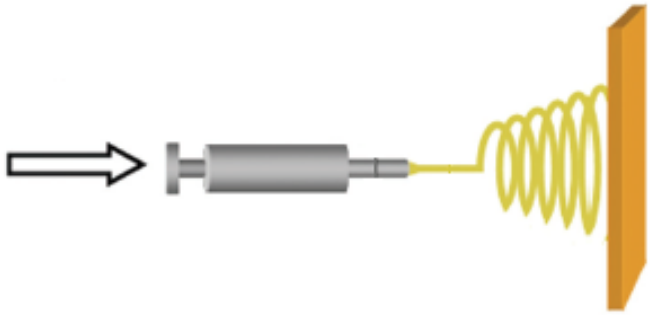

Fig.A1. 1 - Schematic ilustration of electrospinning stratic target set up used in the preleminarie experiments (adapted from [23])

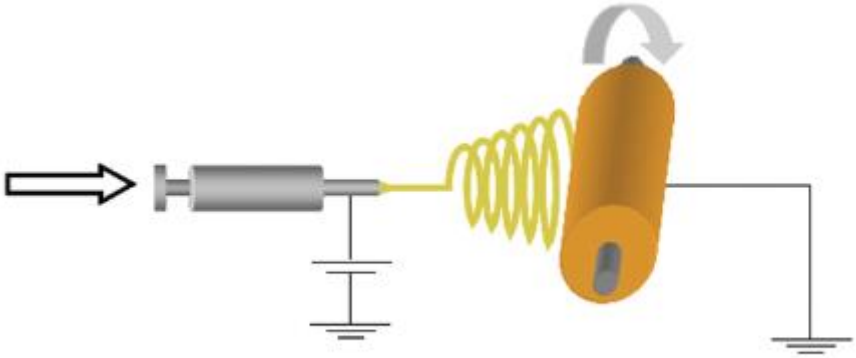

Fig.A1. 2 - - Schematic ilustration of rottating collector drum electrospinning set up used in the production of aligned PVDF fibers. (taken from [23])

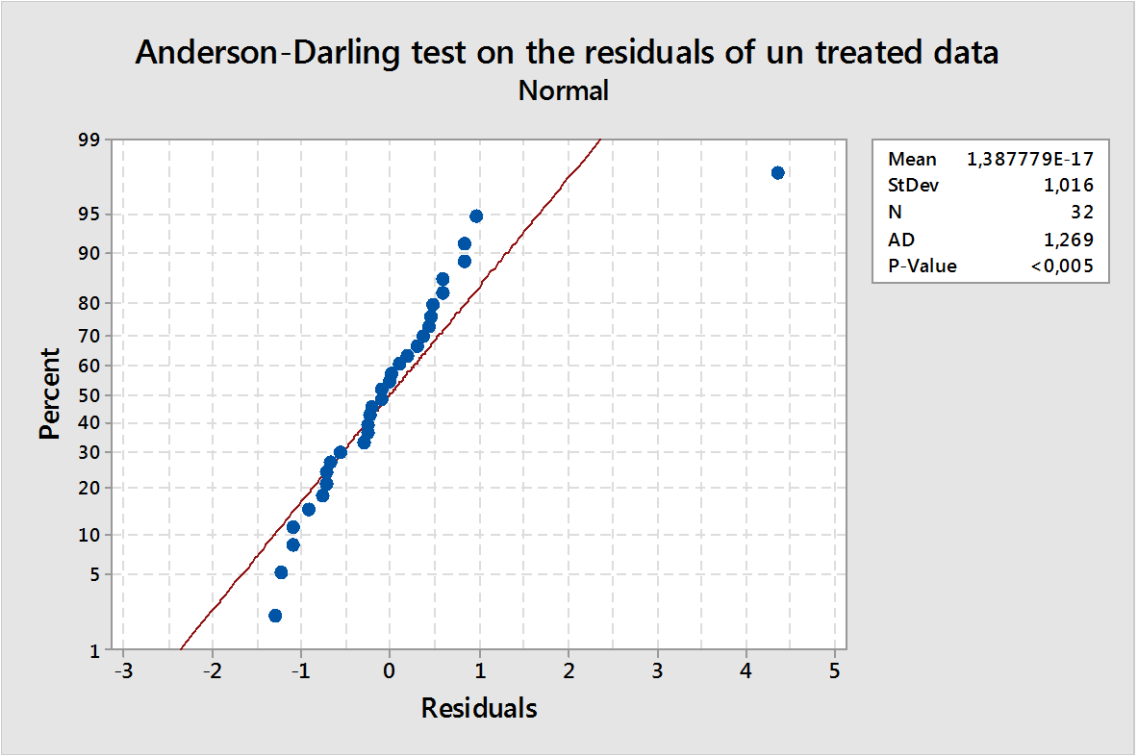

Fig.A2. 1- Graphic representation of the residuals for non-treated data showing a p-value < 0.005

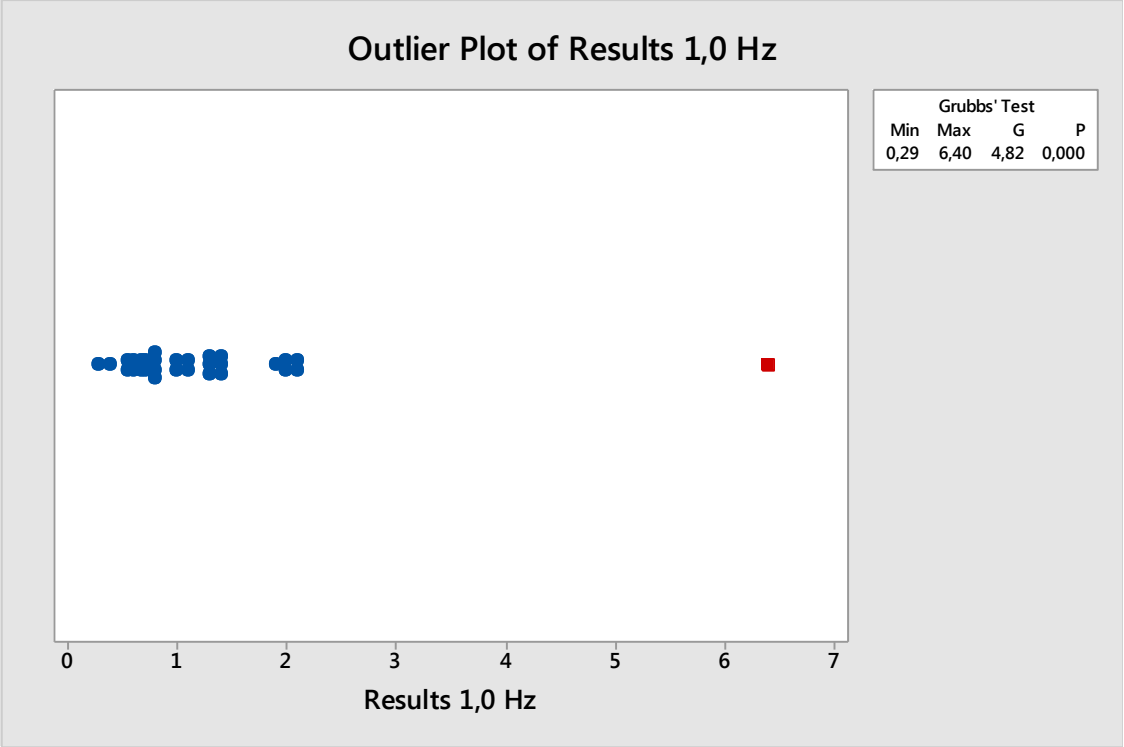

Fig.A2. 2 Grubs test for outliers showing an outlier for a significance level of 0.05, for experiment 17 in the running order with a value of 6.4

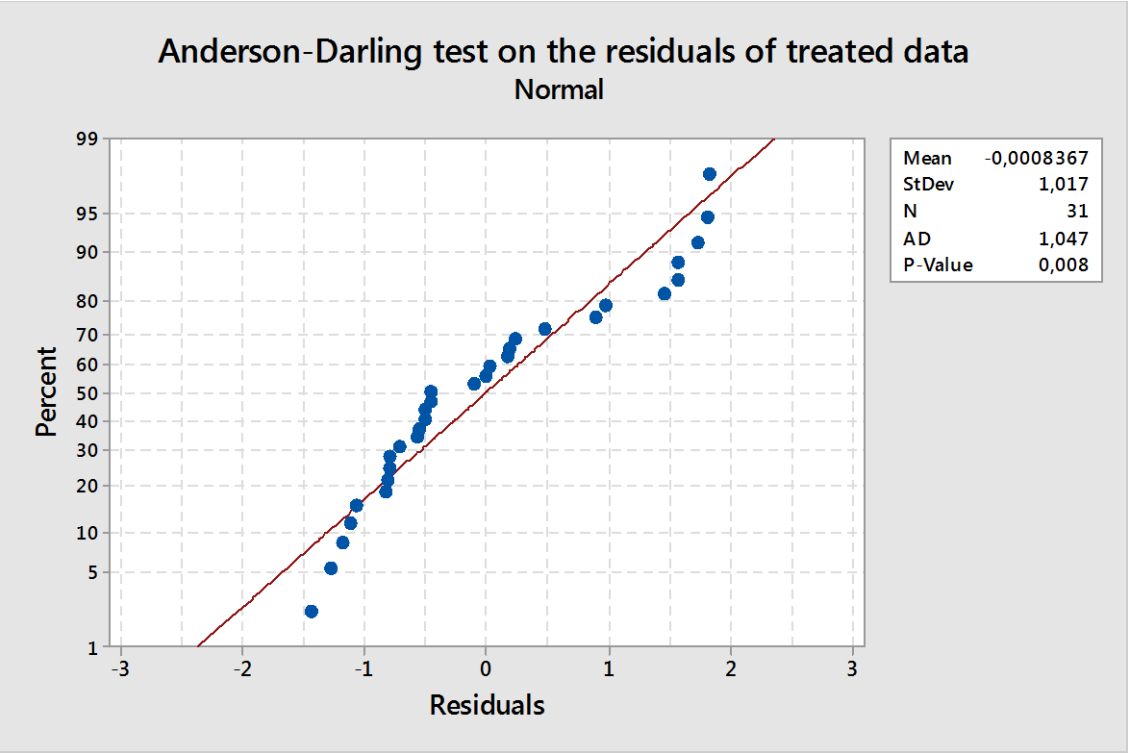

Fig.A2. 3 Graphic representation of the residuals for treated data, showing a p-value > 0.005

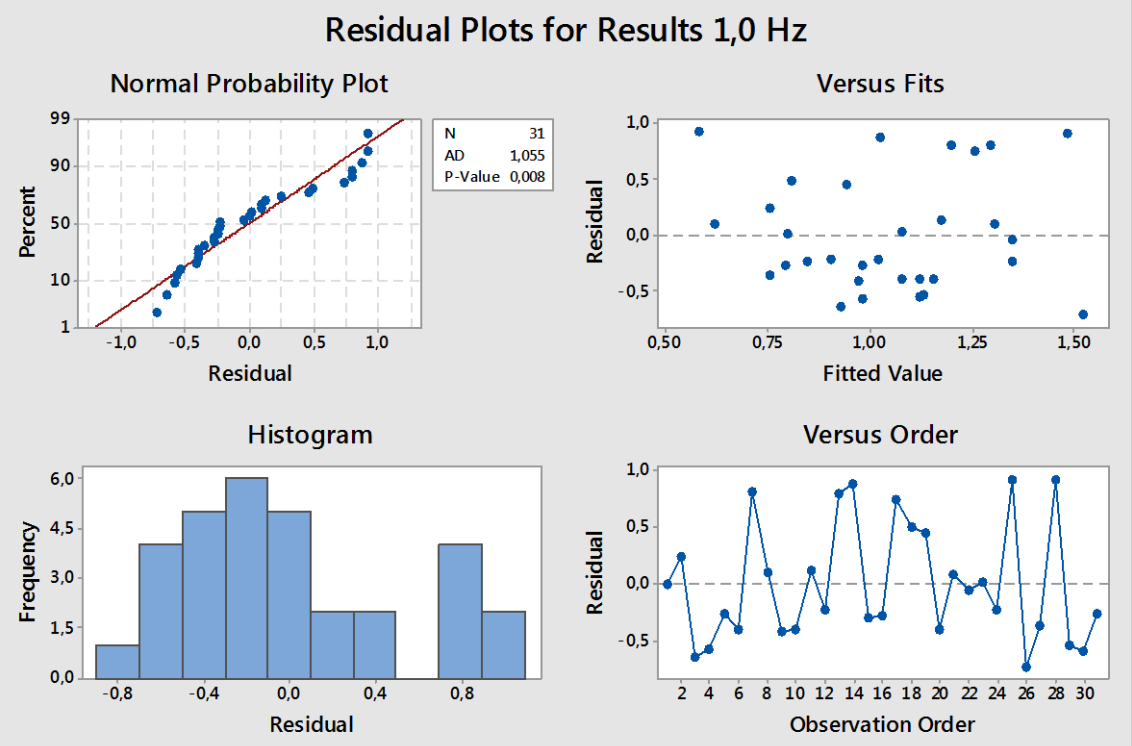

Fig.A2. 4– Residual plots for non-transformed data showing how well they fit a normal distribution, their orde versus the run order and their variance when compared with the fitted values as well as an histogram of their distribuition

3 – Vibration modes of the various peaks of PVDF spectrum.

Experimental Wavenumber, cm^{-1}	Group	Vibration	Comments
3016	CH_2	Symmetric stretching	
2978	CH_2	Asymmetric stretching	
1453	CH_2	In-plane bending or scissoring	
1335	CH_2	Out-of-plane bending (wagging or twisting)	
840	CH_2, CF_2	CH_2 rocking and CF_2 asymmetric stretching	β-Phase (out-of-phase combination)
763		In-plane bending or rocking	α-Phase
745		In-plane bending or rocking	β-Phase
677			Presence of head-to-head and tail-to-tail configurations
615	CF_2, CCC	CF_2 bending and CCC skeletal vibration	α-Phase (out of phase)
600			β-Phase
510	CF_2	Bending	β-Phase
490	CF_2	Bending and wagging	α-Phase (in-phase combination)
445			β-Phase

Fig.A3 1 - Vibrational modes of different peaks present in PVDF FTIR spetrum (taken from [42])

Table A3. 1 - Numerical values for the parameters used in the calculation of molar ohase fraction of the α and β-phases in both ABCE and CE samples

	ABCE	CE	PVDF Powder
A_{762}	0.0238	0.0295	0.0250
A_{1070}	0.2746	0.2641	0.2599
A_{1275}	0.1899	0.1749	0.0649

4 – Results of the Chi-square hypothesis tests for equal variance in proliferation rates from days 3 to 9, after culture, for both ABCE and CE samples

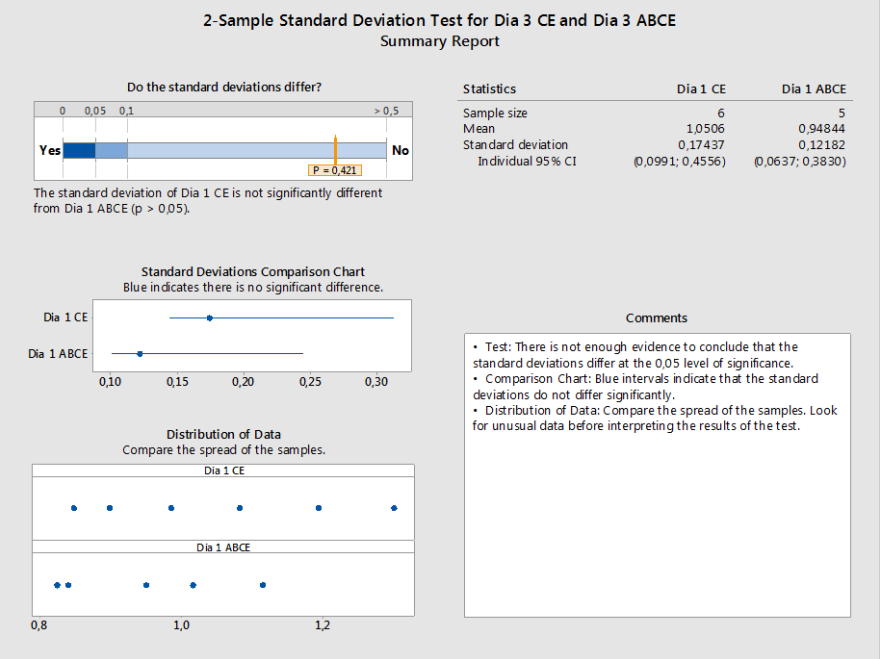

Fig.A4. 1 Two sample Standard deviation test, using a Chi-square statistic for day 3 after culture

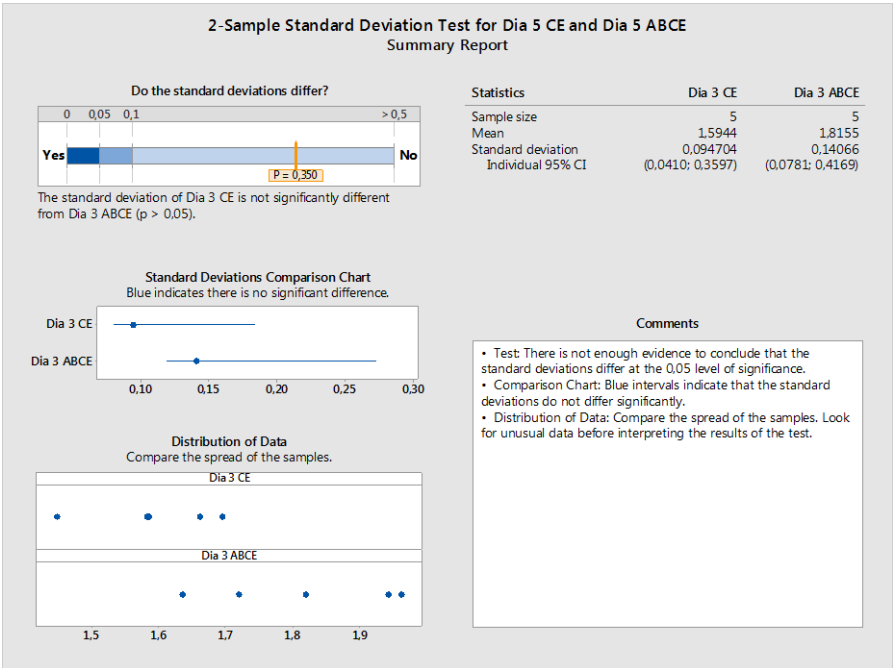

Fig.A4. 2 Two sample Standard deviation test, using a Chi-square statistic for day 5 after culture

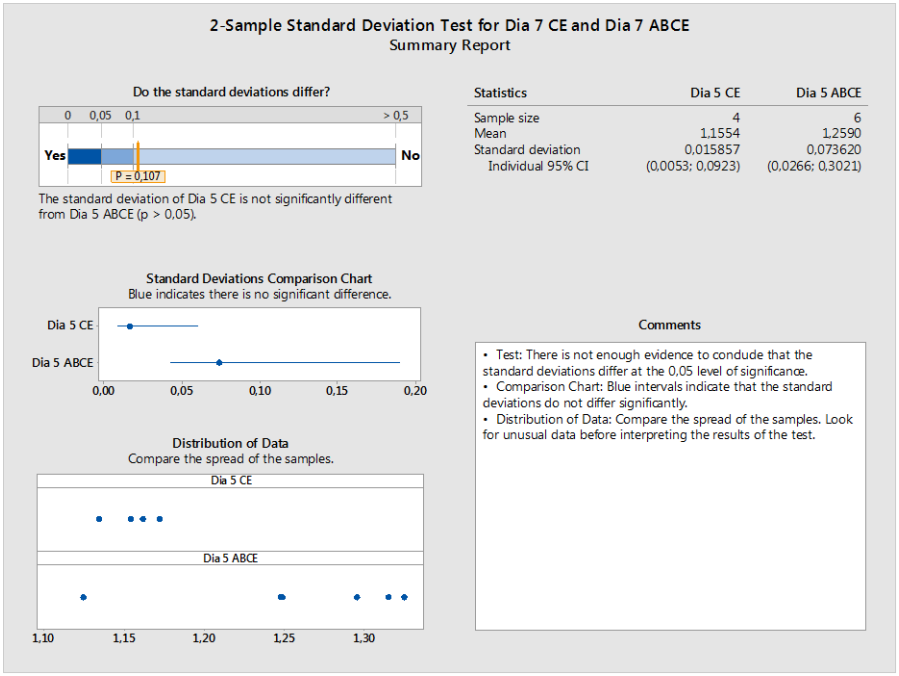

Fig.A4. 3 Two sample Standard deviation test, using a Chi-square statistic for day 7 after culture

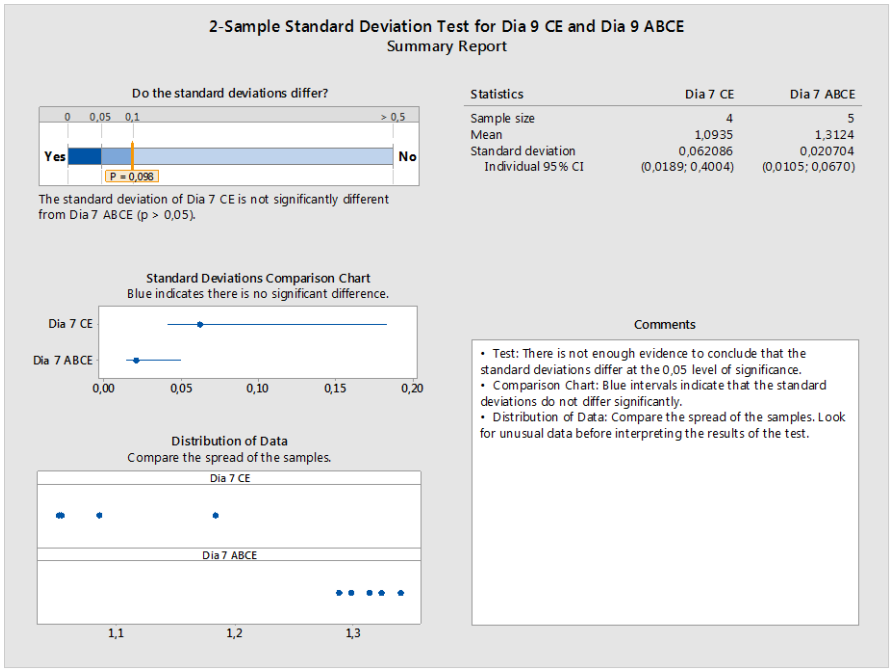

Fig.A4. 4 Two sample Standard deviation test, using a Chi-square statistic for day 9 after culture

5 – Results of the Chi-square hypothesis tests for equal variance for *p*-nitrophenol in both samples and control group

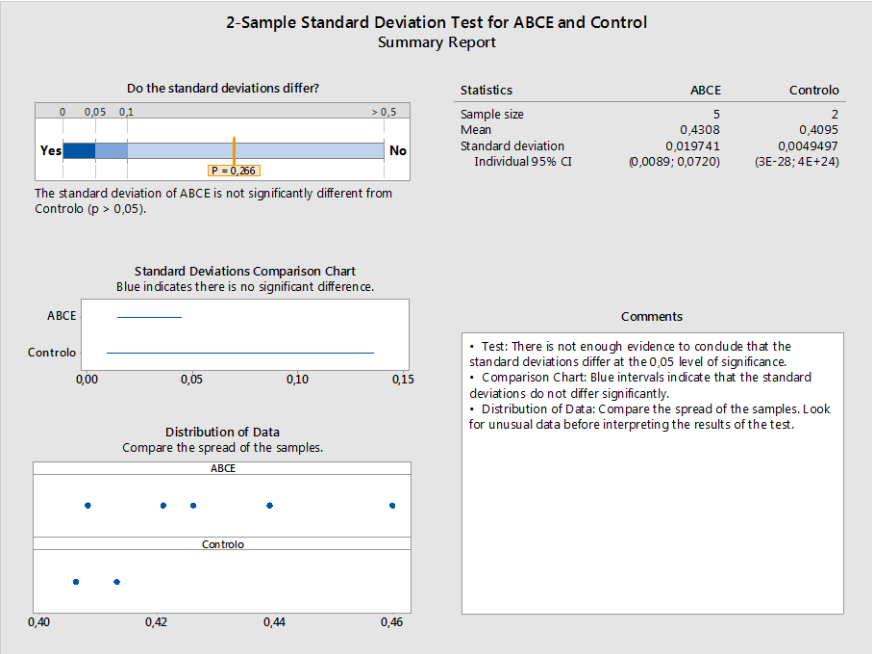

Fig.A5. 5 - Two sample Standard deviation test, using a Chi-square statistic for alkaline phosphatase test between the ABCE and Control groups

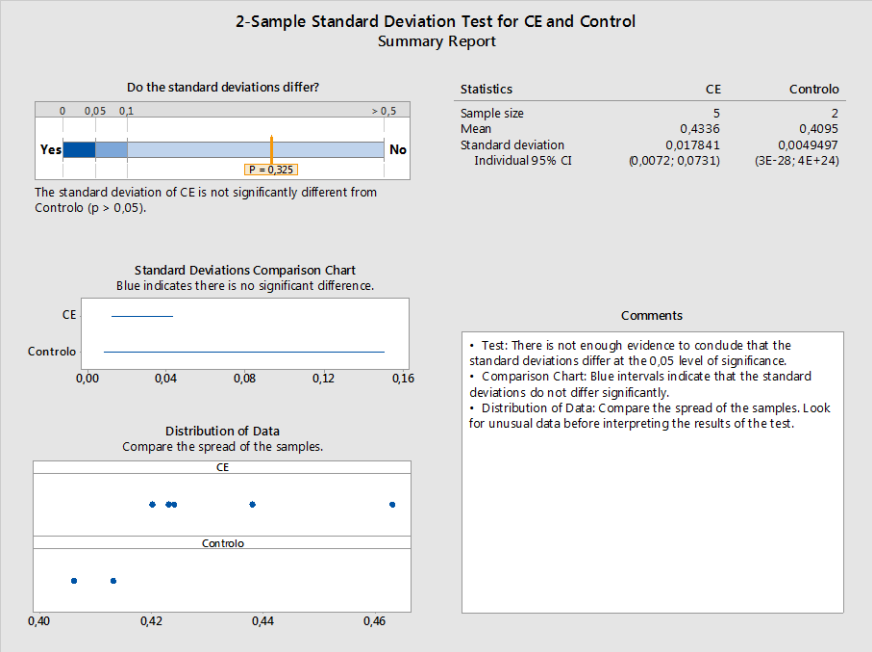

Fig.A5. 6 - Two sample Standard deviation test, using a Chi-square statistic for alkaline phosphatase test between the CE and Control groups

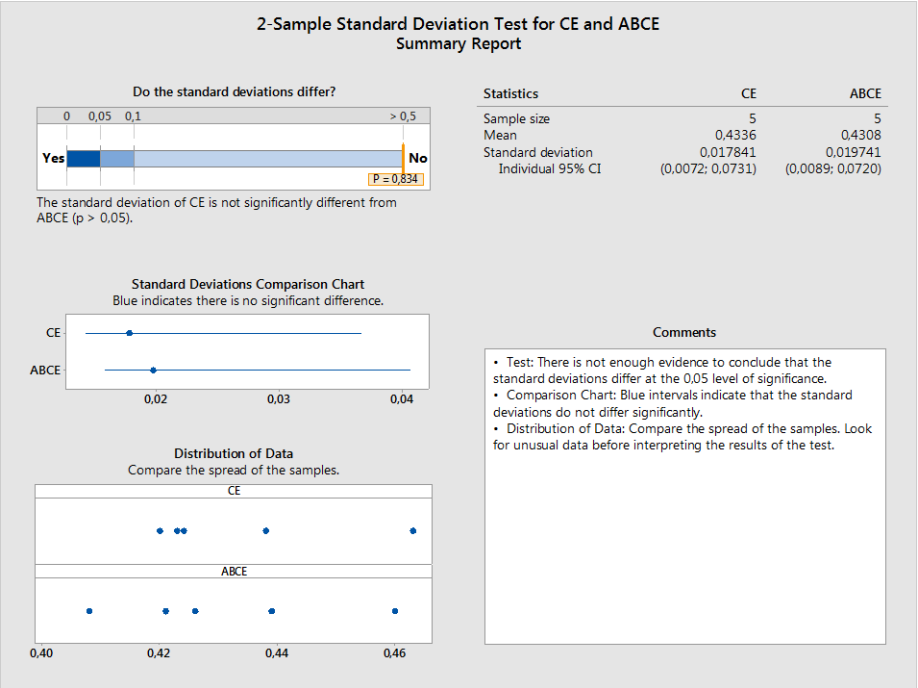

Fig.A5. 7 - Two sample Standard deviation test, using a Chi-square statistic for alkaline phosphatase test between the ABCE and CE groups

6-Bioreactors used in cellular culture tests

Fig.A6 1 - Assembled and disassembled bioreactors used in cellular culture assays